Design and Performance Evaluation of Bitwise Retransmission Schemes in Wireless Sensor Networks

Mohamed A. M. Hassanien[a], Pavel Loskot[a,*], Salman M. Al-Shehri[a],
Tolga Numanoğlu[b], and Mehmet Mert[b]

[a]*College of Engineering, Swansea University, Bay Campus, Swansea SA1 8EN, United Kingdom*
[b]*Aselsan A.S., Communications and IT Division, Ankara, Turkey*

Abstract

The previously proposed bitwise retransmission schemes which retransmit only selected bits to accumulate their reliability are designed and evaluated. Unlike conventional automatic repeat request (ARQ) schemes, the bitwise retransmission schemes do not require a checksum for error detection. The bitwise retransmission decisions and combining can be performed either after demodulation of the received symbols or after channel decoding. The design and analysis assume error-free feedback, however, the impact of feedback errors is also considered. The bit-error rate (BER) expressions are derived and verified by computer simulations in order to optimize the parameters of the retransmission schemes. The BER performance of coded and uncoded bitwise retransmissions is compared with a hybrid ARQ (HARQ) scheme over additive white Gaussian noise (AWGN), slow fading, and fast fading channels. It is shown that bitwise retransmissions outperform block repetition coding (BRC) over AWGN channels. In addition, the selection diversity created by the bitwise retransmissions can outperform the HARQ at large signal-to-noise ratio (SNR) over fast fading channels. Finally, the practical design of a bitwise retransmission protocol for data fusion in wireless sensor networks is presented assuming Zigbee, WiFi and Bluetooth system parameters.

Keywords: Automatic repeat request (ARQ); data fusion; feedback; performance analysis; selection diversity.

1. Introduction

It is well-known that feedback cannot improve the information theoretic capacity of memoryless channels [1]. However, the availability of feedback can greatly simplify the encoding and decoding complexity [2]. A good example of such schemes with reduced implementation complexity due to feedback are ARQ schemes [3, 4]. These schemes are critical for establishing the reliable links in

*Corresponding author: Pavel Loskot, email: p.loskot@swan.ac.uk, tel.: +44 1792 602619, fax: +44 1792 295676

modern communication systems [5, 6, 7].

The retransmission schemes can be optimized to trade-off the reliability (e.g., the BER), throughput (or equivalently, delay), and the implementation complexity [8] or energy consumption [9]. In order to improve the retransmission efficiency, the variable-rate retransmission schemes optimize either the number of retransmissions, or the number of bits in each retransmission [10, 11, 12]. In particular, the incremental redundancy hybrid ARQ (IR-HARQ) or type-II HARQ schemes progressively reduce the coding rate of the forward error correction (FEC) code with each additional retransmission at the expense of increasing the decoding delay and reducing the throughput [13]. Since the received packets typically contain only a few transmission errors, another strategy is to assume partial ARQ schemes [14]. The transmission powers of ARQ schemes are optimized in [11].

The retransmission decision delays in HARQ schemes were reduced in [15] by exploiting the structure of tail-biting convolutional codes. The permutations of bits in the retransmitted packets are used in [16] and [17] to improve the reliability of ARQ schemes. A holistic design of the complexity-constrained type-II hybrid ARQ schemes with turbo codes is considered in [18]. The joint design of FEC coding for the forward data delivery and reverse feedback signaling is studied in [19] and [20]. The IR diversity and the time-repetition diversity are compared in [11]. The time and superposition-coding packet sharing between two independent information flows is evaluated in [21]. It is shown that transmission sharing strategies can significantly outperform the conventional HARQ schemes when the SNR is sufficiently large.

A truncated type II hybrid ARQ over block fading channels is considered in [22]. The number of retransmitted bits required for a successful decoding is estimated from the mutual information in [12] and [21]. The pre-defined retransmission bit-patterns are assumed in [14]. A multi-bit feedback signaling to improve the ARQ performance is considered in [23] and in [21]. More realistic ARQ designs assume noisy feedback [22, 11], and even channel estimation errors [14]. The repetition diversity appears to be more robust to feedback errors than the HARQ [11].

The bitwise retransmission schemes originally devised in our conference paper [23] exploit a multi-bit error-free feedback to trade-off the transmission throughput with the reliability. These schemes were found to outperform stop-and-wait ARQ over an AWGN channel. The complexity can be reduced by considering bit segments instead of individual bits at the cost of sacrificing the performance. Since the data packets often have a fixed length, it is useful to predetermine the number of retransmitted bits as well as the number of retransmissions in order to achieve the constant transmission delay and throughput. Furthermore, unlike the conventional ARQ and HARQ schemes, the

cyclic redundancy check bits are not required in our scheme to make the retransmission decisions.

In this paper, we revisit the bitwise retransmission schemes from [23] to provide more rigorous performance analysis and optimize their design not only for AWGN channels, but also for slow and fast fading channels. The analysis yields a number of new propositions to facilitate the designs of bitwise retransmission schemes. Our analysis assumes a multi-bit error-free feedback signaling, however, we also evaluate the conditions when such assumption is justifiable. The BER performance is evaluated analytically over AWGN and slow fading channels, and by computer simulations over the fast fading channel. We also consider the case of FEC coding combined with the bitwise retransmissions where the bit reliability can be evaluated either before or after the FEC decoding. We show that the FEC coded bitwise retransmissions can outperform the conventional HARQ in fast fading channels due to the inherent selection diversity gain in addition to accumulating the reliability of received bits by the diversity combining. Furthermore, the bitwise retransmission protocol design is illustrated for the wireless sensor network with a star topology and a single data fusion center.

The rest of this paper is organized as follows. System model is introduced in Section 2. Mathematical analysis of the bitwise retransmission schemes is carried out in Section 3. The bitwise retransmission protocols are presented and optimized in Section 4. The performances of the bitwise retransmission schemes and the HARQ scheme over slow and fast fading channels are compared in Section 5. The bitwise ARQ protocol for the uplink data fusion in a wireless sensor network is designed in Section 6. Conclusion is given in Section 7.

2. System Model

The design and analysis of bitwise retransmission schemes is first performed for a point-to-point duplex communication link between a source and a destination assuming the error-free feedback. The effect of feedback errors will be considered in Section 4. The received M-ary modulation symbol s can be written as,

$$y = hs + w$$

where $h > 0$ is a known attenuation, possibly after the multipath equalization, and w is the sample of a zero-mean AWGN. The reliability of the received bit b_i contained in the transmitted symbol s prior to the FEC decoding is calculated as [24],

$$\Lambda(b_i|y) = \log \frac{\Pr(b_i = 0|y)}{\Pr(b_i = 1|y)},\ i = 1, 2, \ldots, \log_2 M. \tag{1}$$

The log-likelihood ratio (LLR) (1) can be rewritten as,

$$\Lambda(b_i|y) = \log \frac{\sum_{s\in S(b_i=0)} \exp\left(-|y-hs|^2/N_0\right)}{\sum_{s\in S(b_i=1)} \exp\left(-|y-hs|^2/N_0\right)} \tag{2}$$

where the M-ary modulation constellation is partitioned by the i-th bit b_i as, $S = S(b_i = 0) \cup S(b_i = 1)$, N_0 is the power spectral density of the AWGN, and $|\cdot|$ denotes the absolute value. The LLR values can be used as the soft-decision inputs to the FEC decoder. In this case, the sums in (2) are done over the corresponding codewords mapped to the sequences of M-ary modulation symbols, and the decoder soft-decision outputs can be used to make the bitwise retransmission decisions. The sums in (2) are often simplified using the formula, $\log \sum_i \exp(-a_i) \approx \min(a_i)$.

In order to make the mathematical analysis tractable, we assume that the fading coefficient h is constant. With sufficient interleaving, the bit errors can be assumed to be independent, even for slowly fading channels. For simplicity, we assume a binary antipodal modulation with the energy per bit, E_b, so the modulation symbols $S_1 = \sqrt{E_b}$ and $S_2 = -\sqrt{E_b}$.

The received N-bit packet can be written as,

$$r_i = S_{ji} + w_i,\ i = 1, 2, \ldots, N$$

where $S_{ji} \in \{S_1, S_2\}$, and the zero-mean AWGN samples w_i have the constant variance, $\mathrm{E}\left[|w_i|^2\right] = \sigma_w^2 = N_0/(2|h|^2)$. Then, the reliability of the received bits are [24],

$$\Lambda(b_i|r_i) \propto |r_i/\sigma_w| \equiv |\bar{r}_i|.$$

The SNR is defined as $\gamma_\mathrm{b} = E_\mathrm{b}/N_0$. Let R_f denote a fraction of information bits in the sequence of all bits transmitted from the source to the destination. For a fair comparison of different bitwise retransmission schemes with various rates R_f, the SNR is further normalized as, $\gamma_\mathrm{b} = E_\mathrm{b} R_\mathrm{f}/N_0$.

2.1. Bitwise retransmissions

After the initial transmission of a N-bit data packet, the destination uses the received bit reliability to report the W_d least reliable bits to the source, so they can be retransmitted where $0 \le W_d \le N$, and $d = 1, 2, \ldots, D$ is the retransmission index. The retransmission request is a feedback message of $C_d \ge 1$ bits sent from the destination to the source over a reverse (feedback) link. Consequently, after the D retransmissions, the total number of bits sent over the forward link to the destination is,

$$N_\mathrm{f} = N + \sum_{d=1}^{D} W_d$$

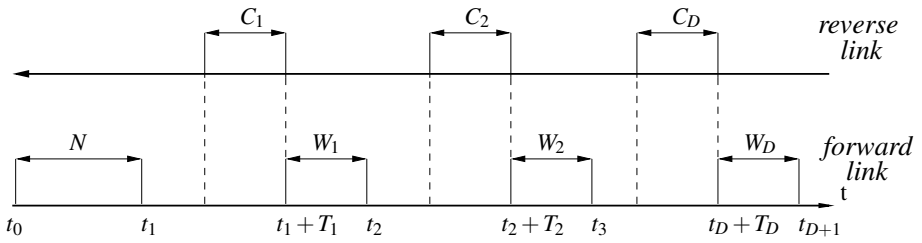

Figure 1: The timings of the bitwise retransmission protocol.

whereas the total number of bits sent from the destination to the source over the reverse link is,

$$N_{\mathrm{r}} = \sum_{d=1}^{D} C_d.$$

This scheme also includes the conventional stop-and-wait ARQ when the parameters $W_d = N$, and $C_d = 1$ represents a ACK or NACK message. The retransmitted bits are combined using a maximum ratio combining (MRC) or any other method to improve their reliability. The timings of the bitwise retransmissions considered in this paper are shown in Figure 1 where T_d represents the delay until the start of the d-th retransmission of W_d bits. The forward transmission rate can be defined as,

$$R_{\mathrm{f}}(D) = \frac{N}{N + \sum_{d=1}^{D} W_d} = \frac{N}{N_{\mathrm{f}}} \tag{3}$$

and the reverse transmission rate is defined as,

$$R_{\mathrm{r}}(D) = \frac{\sum_{d=1}^{D} C_d}{N + \sum_{d=1}^{D} C_d} = \frac{N_{\mathrm{r}}}{N + N_{\mathrm{r}}}.$$

Note that the feedback delays T_d are not included in the definition of these rates, since during these idle time intervals, both forward and reverse links are available for other transmissions.

For simplicity, let $W_1 = W_2 = \ldots = W_D = W$, and $C_1 = C_2 = \ldots = C_D = C$, and we drop the bit index within the packet unless stated otherwise. The W least reliable bits requested for the retransmission can be identified by some sorting algorithm having a typical complexity of $O(N \log N)$ operations [25]. The locations of these W least-reliable bits within the packet of N bits can be reported back to the source by the corresponding binomial number represented by,

$$C = \left\lceil \log_2 \binom{N}{W} \right\rceil$$

bits where $\lceil \cdot \rceil$ denotes the ceiling function. More importantly, even though typically $C > W$, we always have, $R_{\mathrm{f}} \gg R_{\mathrm{r}}$, as in many other ARQ protocols. The multi-bit feedback can be very beneficial to improve the performance of ARQ protocols [23].

3. Performance Analysis

Given the values of N, W, C, D and γ_{b}, our aim is to derive the average BER of the bitwise retransmission schemes. We first assume the case of a single retransmission, i.e., $D = 1$, and optimize the number of feedback message bits C and the forward throughput R_{f} to minimize the BER. The performance is compared to the conventional stop-and-wait ARQ. The BER analysis is then carried out for $D = 2$ retransmissions before it is generalized for $D > 2$ retransmissions.

After a new data packet of N bits was received (i.e., without any retransmissions), the conditional probability density function (PDF) of the received bit reliability $\bar{r}$ is given by,

$$\begin{aligned} \mathrm{f}_{\bar{\mathrm{r}}}(\bar{\mathrm{r}}|\mathrm{S}_1,\mathrm{D}=0) &= \frac{1}{2}\sqrt{\frac{N_o}{\pi}}\,\mathrm{e}^{-\frac{(\bar{r}N_o-2\sqrt{E_b})^2}{4N_o}} \\ \mathrm{f}_{\bar{\mathrm{r}}}(\bar{\mathrm{r}}|\mathrm{S}_2,\mathrm{D}=0) &= \frac{1}{2}\sqrt{\frac{N_o}{\pi}}\,\mathrm{e}^{-\frac{(\bar{r}N_o+2\sqrt{E_b})^2}{4N_o}}. \end{aligned}$$

Since the bits are selected for retransmission based on their reliability, it is useful to derive the BER conditioned on the reliability interval, $L_d \le |\bar{r}| \le U_d$, where the constants $U_d \ge L_d \ge 0$. This BER is equal to the probability of the error event 'e' that S_1 was transmitted, however, S_2 is decided at the receiver when $-U_d \le \bar{r} \le -L_d$. We have that, with no retransmissions,

$$\begin{aligned} \Pr(\mathrm{e}|S_1,D=0) &= \Pr\left(-U_0 \le \bar{r} \le -L_0 \,\middle|\, S_1\right) = \int_{-U_0\sqrt{E_b}}^{-L_0\sqrt{E_b}} \mathrm{f}_{\bar{\mathrm{r}}}(\bar{\mathrm{r}}|\mathrm{S}_1,\mathrm{D}=0)\,\mathrm{d}\bar{r} \\ &= Q\left(\sqrt{2\gamma_{\mathrm{b}}}\left(\frac{L_0}{2\gamma_{\mathrm{b}}}+1\right)\right) - Q\left(\sqrt{2\gamma_{\mathrm{b}}}\left(\frac{U_0}{2\gamma_{\mathrm{b}}}+1\right)\right) \end{aligned}$$

where $Q(x) = \int_x^\infty \frac{1}{\sqrt{2\pi}}\,\mathrm{e}^{-t^2/2}\,\mathrm{d}t$ is the Q-function. The probability that the reliability of the received bit without any retransmissions is in the interval $L_d \le |\bar{r}| \le U_d$ is computed as,

$$\begin{aligned} \mathrm{P}_{0|S_1} &= \Pr\left(L_0 \le |\bar{r}| \le U_0 \,\middle|\, S_1, D=0\right) \\ &= \int_{-U_0}^{-L_0} \mathrm{f}_{\bar{\mathrm{r}}}(\bar{\mathrm{r}}|\mathrm{S}_1,\mathrm{D}=0)\,\mathrm{d}\bar{r} + \int_{L_0}^{U_0} \mathrm{f}_{\bar{\mathrm{r}}}(\bar{\mathrm{r}}|\mathrm{S}_1,\mathrm{D}=0)\,\mathrm{d}\bar{r} \\ &= Q\left(\sqrt{2\gamma_{\mathrm{b}}}\left(\frac{L_0}{2\gamma_{\mathrm{b}}}+1\right)\right) - Q\left(\sqrt{2\gamma_{\mathrm{b}}}\left(\frac{U_0}{2\gamma_{\mathrm{b}}}+1\right)\right) + \\ &\quad Q\left(\sqrt{2\gamma_{\mathrm{b}}}\left(\frac{L_0}{2\gamma_{\mathrm{b}}}-1\right)\right) - Q\left(\sqrt{2\gamma_{\mathrm{b}}}\left(\frac{U_0}{2\gamma_{\mathrm{b}}}-1\right)\right). \end{aligned}$$

Due to symmetry, we can write, $\Pr(e|S_1,D=0) = \Pr(e|S_2,D=0)$, and, $\mathrm{P}_0 = \mathrm{P}_{0|S_1} = \mathrm{P}_{0|S_2}$.

In the sequel, we assume $L_d = 0$ for $\forall d \ge 0$, and the a priori transmission probabilities, $\Pr(S_1) = \Pr(S_2) = 1/2$. Then, the overall average BER, and the overall probability that $0 \le |\bar{r}| \le U_0$, respec-

tively, can be computed as,

$$\begin{aligned} \mathrm{BER}_0 &= Q\Big(\sqrt{2\gamma_\mathrm{b}}\Big) - Q\Bigg(\sqrt{2\gamma_\mathrm{b}}\left(\frac{U_0}{2\gamma_\mathrm{b}}+1\right)\Bigg) \\ \mathrm{P}_0 &= 1 - Q\Bigg(\sqrt{2\gamma_\mathrm{b}}\left(\frac{U_0}{2\gamma_\mathrm{b}}+1\right)\Bigg) - Q\Bigg(\sqrt{2\gamma_\mathrm{b}}\left(\frac{U_0}{2\gamma_\mathrm{b}}-1\right)\Bigg). \end{aligned}$$

Note that, for $U_0 \to \infty$, the overall average BER converges to the BER of uncoded binary antipodal signaling, i.e., $\mathrm{BER}_0 = Q(\sqrt{2\gamma_\mathrm{b}})$ [3], and $\mathrm{P}_0 \to 1$.

Let Z be the number of bits among N received bits having the reliability, $0 \le |\bar{r}| \le U_0$. The mean value, $\mathrm{E}[Z] = N\mathrm{P}_0$, can be used to optimize the retransmission window size. For example, by letting $W \approx \mathrm{E}[Z]$, we can control the target BER after the first retransmission.

After each retransmission with the subsequent MRC combining, it is convenient to re-scale the received samples to maintain a constant average energy per bit in the received packet. In particular, the received sample after combining the initially received sample $\bar{r}_0$ with the retransmitted and scaled samples $\bar{r}_d$, $d = 1,2,\ldots,D$, can be expressed as,

$$\bar{r}_\mathrm{MRC} = \frac{1}{D+1}\left(\bar{r}_0 + \sum_{d=1}^{D} \bar{r}_d\right).$$

3.1. BER with one retransmission

Without loss of generality, we can assume that the packet of N symbols S_1 have been transmitted. After the initial packet transmission, only those bits that have the reliability $|\bar{r}| \le U_0$ are requested to be retransmitted. After these bits are retransmitted, the received samples are,

$$\bar{r}_\mathrm{MRC} = \begin{cases} \frac{1}{2}(\bar{r}_0 + \bar{r}_1) & \text{for} \quad |\bar{r}_0| \le U_0 \\ \bar{r}_0 & \text{for} \quad |\bar{r}_0| > U_0. \end{cases}$$

The random variable $\bar{r}_0$ has the PDF, $\mathrm{f}_{\bar{\mathrm{r}}}(\bar{\mathrm{r}}|\mathrm{S}_1, \mathrm{D}=0)$, whereas the PDF of $\bar{r}_1$ can be obtained by conditioning on $|\bar{r}_0| \le U_0$. Since the received samples $\bar{r}_0$ and $\bar{r}_1$ are statistically independent, the PDF of $\bar{r}_\mathrm{MRC}$ is given by the convolution (denoted as $*$), i.e.,

$$\mathrm{f}_{\bar{\mathrm{r}}_\mathrm{MRC}}(\bar{\mathrm{r}}|\mathrm{S}_1, \mathrm{D}=1) = \frac{\mathrm{f}_{\bar{\mathrm{r}}}(\bar{\mathrm{r}}|\mathrm{S}_1, \mathrm{d}=0)\phi_1(\bar{r}, U_0)}{\Pr\left(|\bar{r}_0| \le U_0 \,\middle|\, S_1, D=0\right)} * \mathrm{f}_{\bar{\mathrm{r}}}(\bar{\mathrm{r}}|\mathrm{S}_1, \mathrm{d}=0)$$

where

$$\phi_1(\bar{r}, U_0) = \eta(\bar{r}+U_0)\,(1-\eta(\bar{r}-U_0))$$

and $\eta(t)$ is the unit-step function, i.e., $\eta(t) = 1$ if $t \ge 0$, and 0 otherwise. After some straightforward but lengthy manipulations, the PDF of $\bar{r}_\mathrm{MRC}$ can be written as,

$$\mathrm{f}_{\bar{\mathrm{r}}_\mathrm{MRC}}(\bar{\mathrm{r}}|\mathrm{S}_1, \mathrm{D}=1) = \frac{\chi_1(\bar{r}, U_0)}{\Pr\left(|\bar{r}_0| \le U_0 \,\middle|\, S_1, D=0\right)}$$

where we defined the function,

$$\chi_d(\bar{r},U_0)=\frac{1}{4}\sqrt{\frac{(d+1)N_o}{\pi}}\,\mathrm{e}^{-\frac{\left(\bar{r}-2\sqrt{\frac{\gamma_b}{N_o}}\right)^2}{\frac{4}{(d+1)N_o}}}\left\{\mathrm{erf}\left(\sqrt{\frac{(d+1)N_o}{4d}}(U_0-\bar{r})\right)+\mathrm{erf}\left(\sqrt{\frac{(d+1)N_o}{4d}}(U_0+\bar{r})\right)\right\}$$

and $\mathrm{erf}(\cdot)$ denotes the error function [3]. The overall BER_1 after the first retransmission is computed as,

$$\begin{aligned}\mathrm{BER}_1 &= \Pr(e|d=0,S_1)\Pr(d=0|S_1)+\Pr(e|d=1,S_1)\Pr(d=1|S_1)\\ &= \int_{-\infty}^{-U_0}\mathrm{f}_{\bar{\mathrm{r}}}(\bar{\mathrm{r}}|\mathrm{S}_1,\mathrm{d}=0)\,\mathrm{d}\bar{r}+\int_{-\infty}^{0}\chi_1(\bar{r},U_0)\,\mathrm{d}\bar{r}.\end{aligned}$$

The numerically efficient approximation of the BER_1 is provided in Appendix.

3.2. BER with two retransmissions

After the second retransmission, the received bits having the reliability $U_0<|\bar{r}|\le U_1$ are combined with the retransmitted samples $\bar{r}_2$. In particular, the received samples after two retransmissions are,

$$\bar{r}_{\mathrm{MRC}}=\begin{cases}\frac{1}{3}(\bar{r}_0+\bar{r}_1+\bar{r}_2) & \text{for} \quad |\bar{r}_0|\le U_0,\ \frac{1}{2}|\bar{r}_0+\bar{r}_1|\le U_1\\ \frac{1}{2}(\bar{r}_0+\bar{r}_1) & \text{for} \quad |\bar{r}_0|\le U_0,\ \frac{1}{2}|\bar{r}_0+\bar{r}_1|> U_1\\ \frac{1}{2}(\bar{r}_0+\bar{r}_2) & \text{for} \quad U_0<|\bar{r}_0|\le U_1\\ \bar{r}_0 & \text{for} \quad |\bar{r}_0|> U_1.\end{cases} \tag{4}$$

In order to make the analysis mathematically tractable, we merge the first two conditions in (4), and consider instead the retransmission policy,

$$\bar{r}_{\mathrm{MRC}}=\begin{cases}\frac{1}{3}(\bar{r}_0+\bar{r}_1+\bar{r}_2) & \text{for} \quad |\bar{r}_0|\le U_0\\ \frac{1}{2}(\bar{r}_0+\bar{r}_2) & \text{for} \quad U_0<|\bar{r}_0|\le U_1\\ \bar{r}_0 & \text{for} \quad |\bar{r}_0|> U_1\end{cases} \tag{5}$$

representing the upper-bound performance of the scheme in (4). The scheme (5) can be interpreted as making the decision about the retransmissions of each bit already after evaluating the reliability of the initially received bits. The scheme (5) may unnecessarily retransmit some bits even though their reliability has already reached the desired threshold after some retransmission. However, our numerical results indicate that, for $D=2$, the performance difference of schemes (4) and (5) is not significant (less than 0.5 dB). Consequently, the number of retransmissions of each bit assuming the scheme (5) can be determined by quantization of the initial reliability $|\bar{r}_0|$ using the thresholds U_0 and U_1. The initially received bits having the reliability $|\bar{r}_0|\le U_0$ are always combined with two other

retransmitted bits whereas the received bits with the reliability $U_0 < |\bar{r}_0| \leq U_1$ are combined with exactly one retransmission. For this retransmission rule, the PDF of $\bar{r}_{\mathrm{MRC}}$ is computed as,

$$\mathrm{f}_{\bar{\mathrm{r}}_{\mathrm{MRC}}}(\bar{\mathrm{r}}|\mathrm{S}_1,\mathrm{d}=2) = \begin{cases} \frac{\chi_1(\bar{r},U_0)}{\Pr\left(|\bar{r}_0|\leq U_0 \,\middle|\, S_1,d=0\right)} & |\bar{r}| \leq U_0 \\ \mathrm{f}_{\bar{\mathrm{r}}_{\mathrm{MRC}}}(\bar{\mathrm{r}}|\mathrm{S}_1,\mathrm{d}=2) = \frac{\lambda_1(\bar{r},U_1,U_0)}{\Pr\left(U_0<|\bar{r}_0|\leq U_1 \,\middle|\, S_1,d=0\right)} & U_0 < |\bar{r}_0| \leq U_1 \\ \mathrm{f}_{\bar{\mathrm{r}}}(\bar{\mathrm{r}}|\mathrm{S}_1,\mathrm{d}=0) & U_1 < |\bar{r}_0| \end{cases}$$

where

$$\lambda_d(\bar{r},U_d,U_{d-1}) = \tfrac{1}{4}\sqrt{\tfrac{(d+1)N_o}{\pi}}\ \exp\left(-\frac{\left(\bar{r}-2\sqrt{\frac{\gamma_b}{N_o}}\right)^2}{\frac{4}{(d+1)N_o}}\right)\times$$
$$\left\{\mathrm{erf}\left(\sqrt{\tfrac{(d+1)N_o}{4d}}(U_d+\bar{r})\right)+\mathrm{erf}\left(\sqrt{\tfrac{(d+1)N_o}{4d}}(U_d-\bar{r})\right)-\right.$$
$$\left.\mathrm{erf}\left(\sqrt{\tfrac{(d+1)N_o}{4d}}(U_{d-1}+\bar{r})\right)-\mathrm{erf}\left(\sqrt{\tfrac{(d+1)N_o}{4d}}(U_{d-1}-\bar{r})\right)\right\}.$$

The probability that the received reliability is in the interval $U_0 \leq |\bar{r}| \leq U_1$ is evaluated as,

$$\begin{aligned} \mathrm{P}_1 = {} & \Pr\left(|\bar{r}| \leq U_1 \,\middle|\, S_1,d=0\right)\Pr\left(d=0|S_1\right)+ \\ & \Pr\left(|\bar{r}| \leq U_1 \,\middle|\, S_1,d=1\right)\Pr\left(d=1|S_1\right) = \textstyle\int_{-U_1}^{U_1}\mathrm{f}_{\bar{\mathrm{r}}}(\bar{\mathrm{r}}|\mathrm{S}_1,\mathrm{D}=0)\,\mathrm{d}\bar{r} \\ & -\textstyle\int_{U_0}^{U_0}\mathrm{f}_{\bar{\mathrm{r}}}(\bar{\mathrm{r}}|\mathrm{S}_1,\mathrm{D}=0)\,\mathrm{d}\bar{r}+\int_{-U_1}^{U_1}\chi_1(\bar{r},U_0)\,\mathrm{d}\bar{r}. \end{aligned} \tag{6}$$

Since the probability of the second bit retransmission is, $\Pr\left(d=2|S_1\right) = \Pr\left(\bar{r} \leq -U_1 \,\middle|\, S_1,d=1\right)$, the overall BER_2 is calculated as,

$$\begin{aligned} \mathrm{BER}_2 &= \sum_{d=0}^{2}\Pr\left(e|d,S_1\right)\Pr\left(d|S_1\right) \\ &= \int_{-\infty}^{-U_1}\mathrm{f}_{\bar{\mathrm{r}}}(\bar{\mathrm{r}}|\mathrm{S}_1,\mathrm{D}=0)\,\mathrm{d}\bar{r}+\int_{-\infty}^{0}\lambda_1(\bar{r},U_1,U_0)\,\mathrm{d}\bar{r}+\int_{-\infty}^{0}\chi_2(\bar{r},U_0)\,\mathrm{d}\bar{r}. \end{aligned}$$

The numerically efficient approximations of the probability (6) and of the BER_2 are provided in Appendix.

3.3. BER with more than two retransmissions

After $D \geq 2$ retransmissions assuming the thresholds,

$$U_{D-1} \geq U_{D-2} \ldots \geq U_1 \geq U_0$$

the overall BER is calculated as,

$$\mathrm{BER}_D = \sum_{d=0}^{D}\Pr\left(e|d,S_1\right)\Pr\left(d|S_1\right).$$

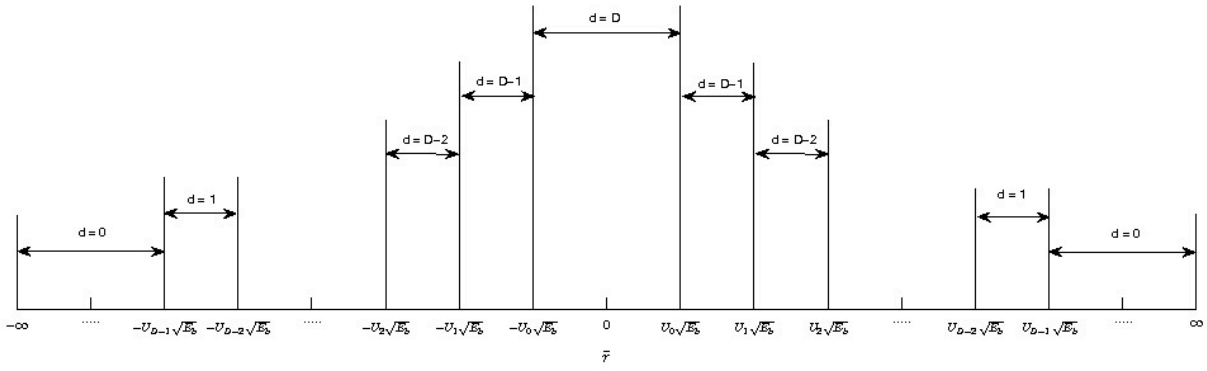

Figure 2: The quantization levels of the bit reliability with D retransmissions.

For the sake of mathematical tractability, we again assume that the received bits having the initial reliability within the interval $|\bar{r}| \leq U_0$ will be retransmitted D times, the bits with the reliability in the interval $U_0 < |\bar{r}| \leq U_1$ will be retransmitted $D-1$ times and so on. The number of received copies for each reliability range after D retransmissions is shown in Figure 2.

The probability P_D that the received reliability is in the interval $U_{D-1} \leq |\bar{r}| \leq U_D$ is evaluated as,

$$\begin{aligned} \mathrm{P}_D &= \int_{-U_D}^{U_D} \mathrm{f}_{\bar{\mathrm{r}}}(\bar{\mathrm{r}}|\mathrm{S}_1, \mathrm{D}=0)\,\mathrm{d}\bar{r} - \int_{-U_0}^{U_0} \mathrm{f}_{\bar{\mathrm{r}}}(\bar{\mathrm{r}}|\mathrm{S}_1, \mathrm{D}=0)\,\mathrm{d}\bar{r} \\ &\quad + \sum_{i=1}^{D-1} \int_{-U_D}^{U_D} \lambda_i(\bar{r}, U_{D-i}, U_{D-i-1})\,\mathrm{d}\bar{r} + \int_{-U_D}^{U_D} \chi_D(\bar{r}, U_0)\,\mathrm{d}\bar{r} \end{aligned}$$

with the third term being zero for $D = 1$ retransmission. It is again possible to obtain the approximation of the probability P_D for $D > 2$. However, the resulting expression is much more evolved than for P_1 and P_2. Consequently, the overall BER can be calculated using the functions $\chi_D(\bar{r}, U_{D-1})$ and $\lambda_D(\bar{r}, U_D, U_{D-1})$ defined in Section 3.1 and 3.2, respectively, i.e.,

$$\mathrm{BER}_D = \int_{-\infty}^{-U_{D-1}} \mathrm{f}_{\bar{\mathrm{r}}}(\bar{\mathrm{r}}|\mathrm{S}_1, \mathrm{D}=0)\,\mathrm{d}\bar{r} + \int_{-\infty}^{0} \chi_D(\bar{r}, U_0)\,\mathrm{d}\bar{r} + \sum_{i=1}^{D-1} \int_{-\infty}^{0} \lambda_i(\bar{r}, U_{D-i}, U_{D-i-1})\,\mathrm{d}\bar{r}$$

where the middle term is zero for $D = 1$ retransmission. The numerically efficient approximation of the BER_D is provided in Appendix.

3.4. BER for time-varying channels

Provided that the SNR variations due to fading are sufficiently slow, so the SNR is approximately constant during each packet transmission, the BER performance for AWGN channel obtained in Sections 3.1–3.3 can be simply averaged over the SNR distribution. If the SNR values are statistically independent, such channel model is referred to as a block fading channel. This model is appropriate

for scenarios with stationary or nomadic mobility of network nodes, and when the packets are relatively short, i.e., either N is small, or the data rate is large. Assuming the chi-square distribution for SNR, $f_{\gamma_b}(\gamma_b) = \frac{1}{\bar{\gamma}_b} \exp\left(-\frac{\gamma_b}{\bar{\gamma}_b}\right)$, where $\bar{\gamma}_b = \mathrm{E}[\gamma_b]$, corresponding to the Rayleigh distributed fading magnitudes h, the approximate average BER over a slowly fading channel after D retransmissions is provided in Appendix.

In scenarios with faster mobility, a sufficient level of bit interleaving can make the fading to be independent for each transmitted bit while still allowing for coherent detection. This channel model is referred to as a fast fading channel. Since the resulting expression of the average BER is rather evolved, the BER performance for fast fading channel is evaluated by computer simulations.

4. Bitwise Retransmission Schemes

We investigate three specific bitwise retransmission strategies and optimize their parameters to maximize the transmission reliability (i.e., minimize the BER) for a given transmission rate. However, the throughput maximization problem is not considered in this paper. We also verify the BER expressions obtained in the previous section by computer simulations assuming error-free feedback. This assumption is revisited at the end of this section.

4.1. Fixed rate technique

In this design, we assume a constant retransmission window size W determined as,

$$W = \left\lceil \frac{N}{D}\left(\frac{1}{R_f} - 1\right) \right\rfloor$$

where $\lceil \cdot \rfloor$ is the rounding function. The parameters N, D and R_f are the design parameters. Since the window size $1 \leq W \leq N$, the feasible forward rate is constrained as, $\frac{1}{1+D} < R_f \leq \frac{N}{D+N}$. For $W = N$, the rate $R_f = \frac{1}{1+D}$, and the retransmission scheme corresponds to a BRC with D repetitions of the original packet. We have the following proposition.

Proposition 1. *For a given SNR, the fixed rate retransmission technique achieves the minimum BER for some specific value of the forward rate R_f. The optimum value of R_f minimizing the BER increases with SNR.*

Proposition 1 can be proved by letting the derivative $(\mathrm{d}/\mathrm{d}R_f)\,\mathrm{BER}_D$ to be equal to zero. For large values of SNR and N, the forward rate R_f approaches its maximum value of 1. In such a case, the overhead due to retransmissions can be neglected. Moreover, when N is large or when $W = N$, the BER of the fixed rate retransmission scheme approaches the BER of the BRC.

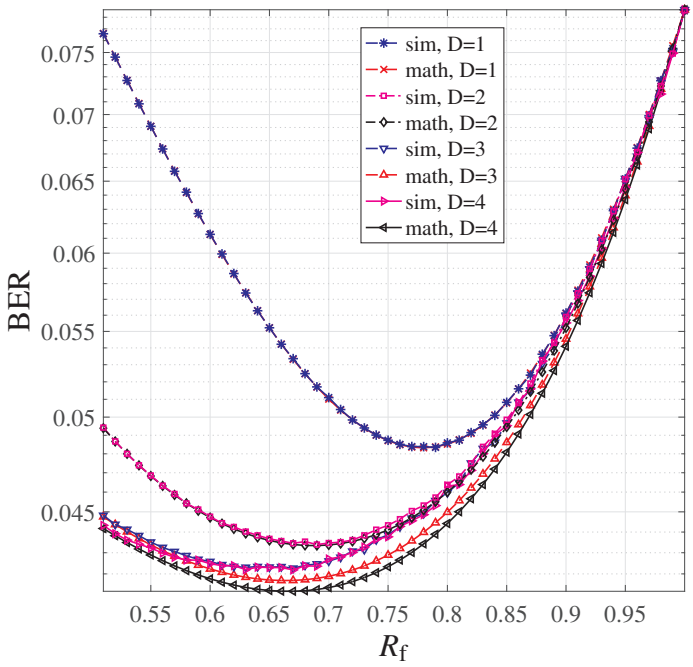

Figure 3: The BER versus the forward rate R_f for $\gamma_{\mathrm{b}} = 0$ dB and the different number of retransmissions D.

Figure 3 and Figure 4 show the BER of the forward link versus the forward rate R_{f} for the different number of retransmissions D at two SNR values $\gamma_{\mathrm{b}} = 0$ dB and $\gamma_{\mathrm{b}} = 5$ dB, respectively. We observe that the minimum BER value is more pronounced (i.e., the optimization is more important) for larger values of SNR. The BER curves in Figure 3 and Figure 4 also compare simulations with the approximate BER expressions given in Appendix. For $D > 1$, the difference between the approximate expressions and the simulations is negligible.

The forward rates R_{f} yielding the minimum BER are shown in Figure 5 for the different number of retransmissions D. Figure 6 shows the BER versus SNR γ_{b} for the different number of retransmissions D assuming that the forward rate R_{f} is optimized for each SNR value γ_{b} to minimize the achieved BER. Note that such optimization becomes more effective if SNR is increased. We observe that the optimized bitwise retransmission scheme with $D \geq 1$ retransmissions and the rate $R_f > 1/2$ provides at least 3.2 dB gain over the rate $1/2$ BRC; however, the gain appears to diminish quickly with the increasing number of retransmissions D.

4.2. Fixed window technique

As for the fixed rate technique, the retransmission window size is fixed, and it is determined as,

$$W = \lceil NP \rfloor .$$

The retransmission decision thresholds U_d are set to make the probabilities, $P = \mathrm{P}_0 = \mathrm{P}_1 = \ldots = \mathrm{P}_{D-1}$, equal. These probabilities were determined in the previous section. Then, given the design parameters

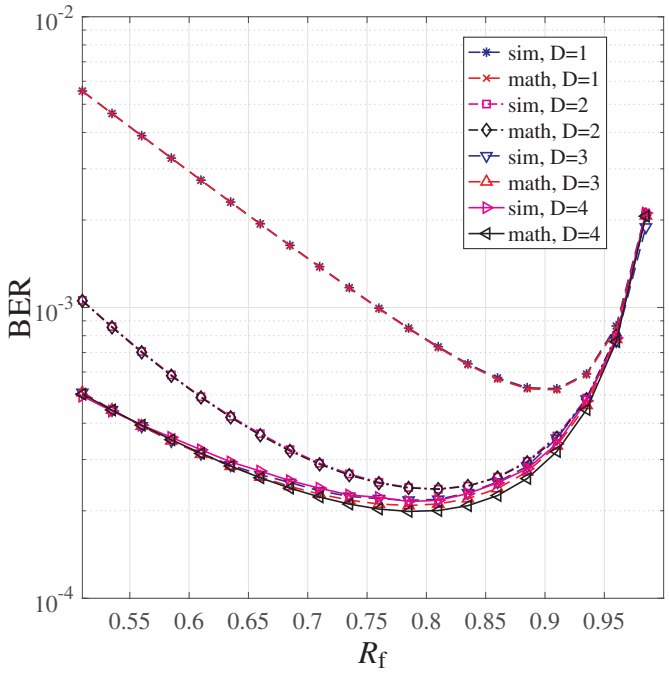

Figure 4: The BER versus the forward rate R_f for $\gamma_{\mathrm{b}} = 5$ dB and the different number of retransmissions D.

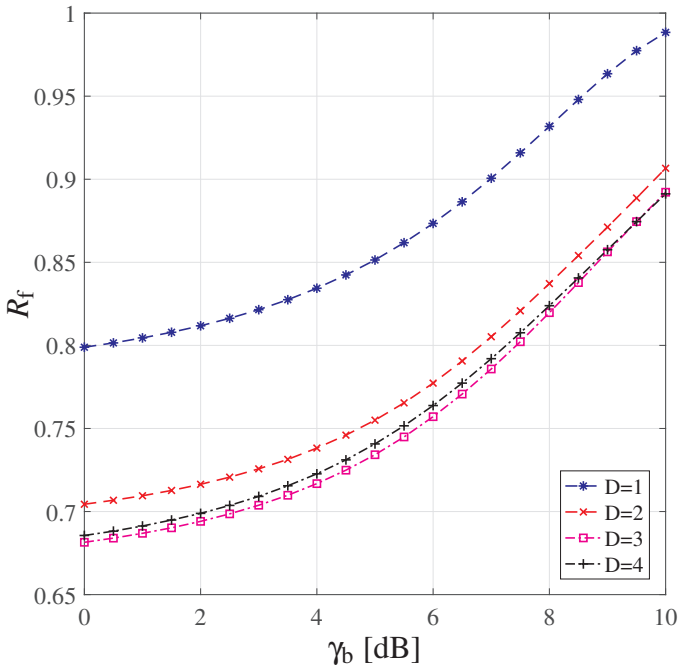

Figure 5: The rate R_f yielding the minimum BER versus the SNR γ_{b} for the different number of retransmissions D.

N, D and W, the forward rate is calculated as,

$$R_{\mathrm{f}} = \frac{1}{1+DW/N}.$$

We have the following proposition.

Proposition 2. *For a given SNR, the fixed window technique achieves the minimum BER for some*

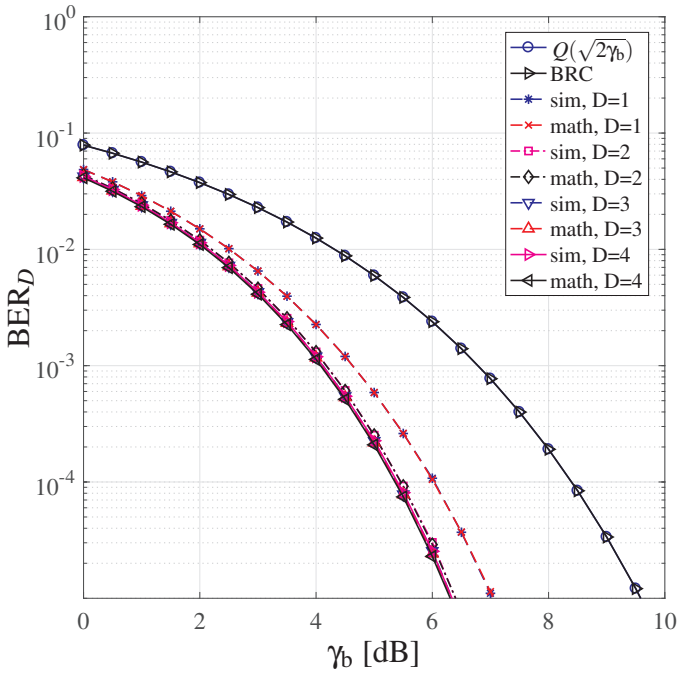

Figure 6: The BER_D versus the SNR γ_b for the different number of retransmissions D.

value of the retransmission window size. The optimum retransmission window size decreases with SNR.

Assuming a fractional window size $W = NP > 0$, Proposition 2 can be again proved by letting the derivative, $(\mathrm{d}/\mathrm{d}W)\,\mathrm{BER}_D$ to be equal to zero. For $W \to N$, the BER of the fixed window technique approaches the BER of BRC. In general, the retransmission overhead can be neglected, if $W \ll N$.

Figure 7 and Figure 8 show the BER versus the normalized window size W/N for the different number of retransmissions D and the SNR values $\gamma_b = 0$ dB and $\gamma_b = 5$ dB, respectively. We again observe a negligible difference between the approximate and the simulated BER curves, especially for larger values of D. In addition, the minimum BER values are more pronounced when the SNR is increased.

Figure 9 shows the normalized window size W/N corresponding to the minimum BER for the different number of retransmissions D. Figure 10 shows the BER versus the SNR γ_b for the different number of retransmissions D assuming the optimum value of W/N for each γ_b minimizing the BER. Note that such minimization of the BER is again more effective when the SNR is large. The performance of this bitwise retransmission scheme appears to be similar as in Figure 6.

4.3. Fixed threshold technique

Unlike the previous two techniques, the fixed threshold technique allows for the different retransmission window sizes while assuming constant reliability thresholds, $U_0 = U_1 = \ldots = U_{D-1} = U$,

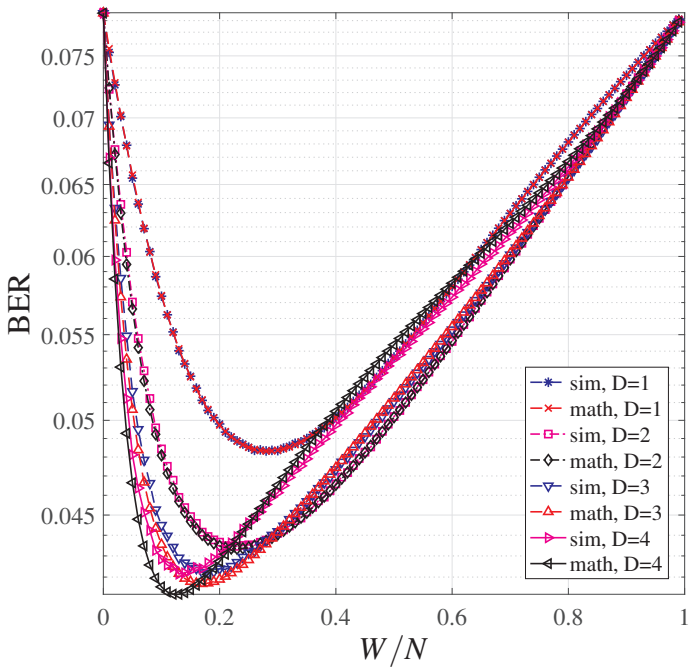

Figure 7: The BER versus the normalized window size W/N for $\gamma_b = 0$ dB and the different number of retransmissions D.

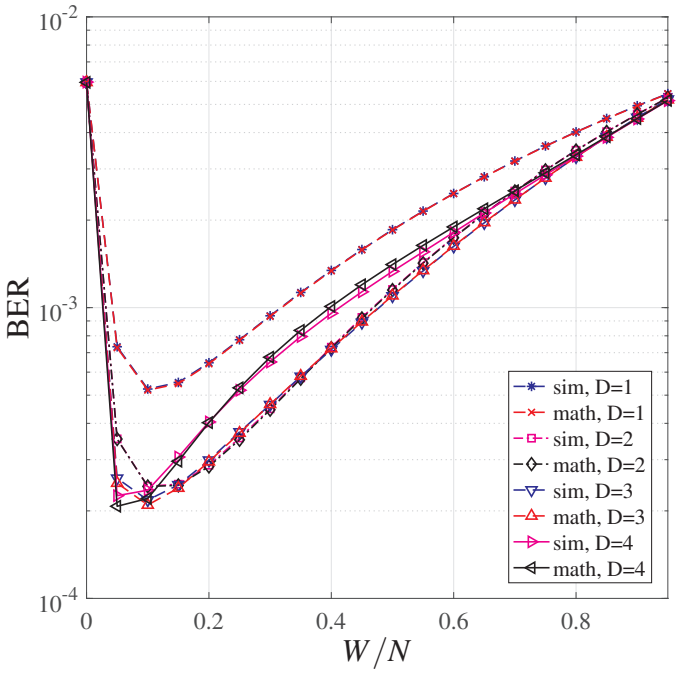

Figure 8: The BER versus the normalized window size W/N for $\gamma_b = 5$ dB and the different number of retransmissions D.

during each retransmission. Given U, we obtain the probabilities P_d, $d = 1,2,\ldots,D$, defined previously to calculate the retransmission window sizes as,

$$W_d = \lceil NP_d \rfloor .$$

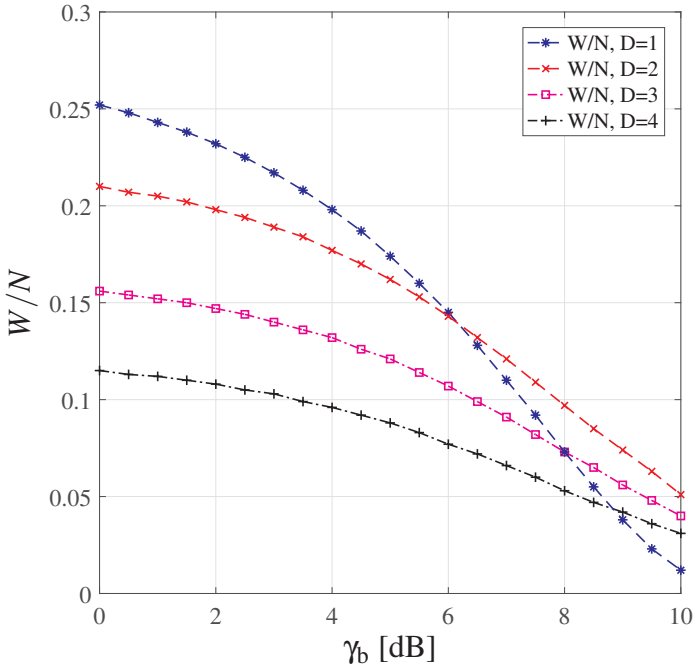

Figure 9: The normalized window size W/N yielding the minimum BER versus SNR γ_b for the different number of retransmissions D.

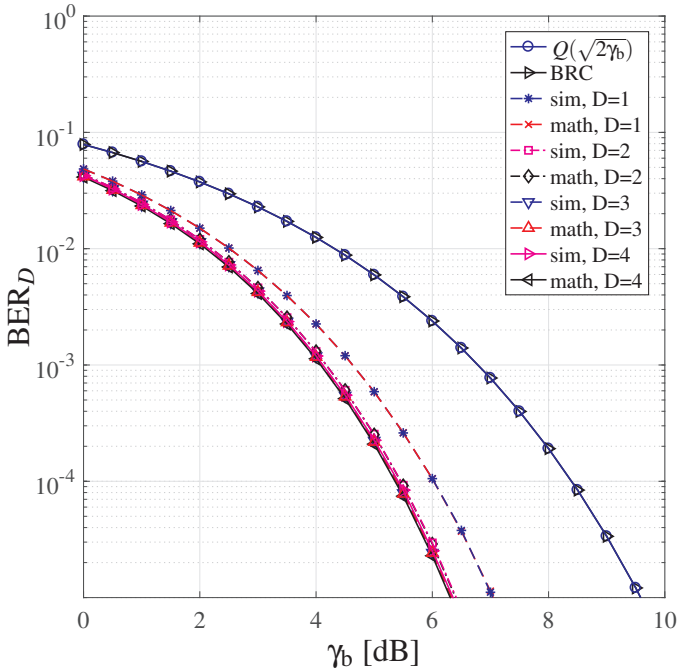

Figure 10: The BER_D versus SNR γ_b for the different number of retransmissions D.

The corresponding forward rate is calculated as,

$$R_{\mathrm{f}} = \frac{1}{1+\sum_{d=1}^{D} W_d/N}.$$

We have the following proposition.

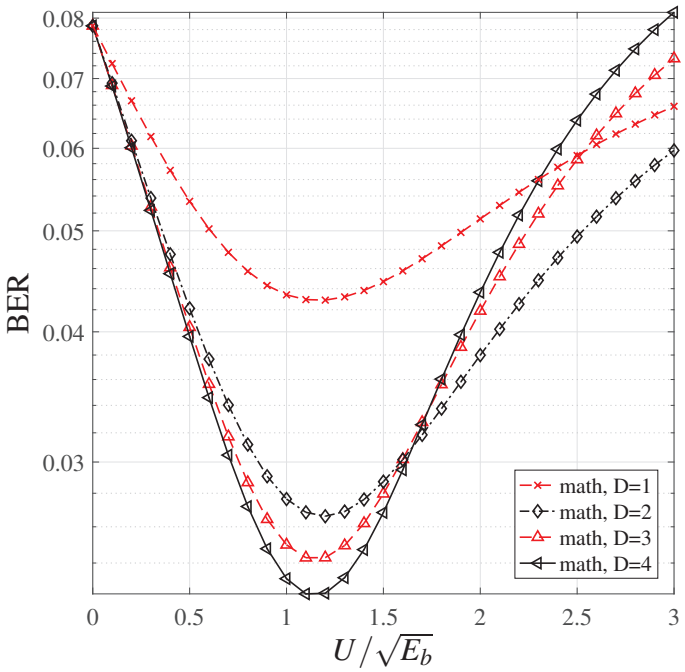

Figure 11: The BER versus the normalized threshold $U/\sqrt{E_b}$ for the SNR $\gamma_b = 0$ dB and the different number of retransmissions D.

Proposition 3. *For a given SNR, the fixed threshold technique achieves the minimum BER value for some specific threshold U. This optimum threshold value is increasing with SNR.*

Proposition 3 can be again proved by letting the derivative, $(\mathrm{d}/\mathrm{d}U)\,\mathrm{BER}_D$ to be equal to zero.

Figure 11 and Figure 12 show the BER versus the normalized threshold $U/\sqrt{E_b}$ for the different number of retransmissions D and the SNR values $\gamma_b = 0$ dB and $\gamma_b = 5$ dB, respectively. Since the approximate BER expressions were already verified for the other two bitwise retransmission techniques, the BER curves in Figure 11 and Figure 12 only show these derived expressions. We observe that the minimum BER values are more apparent when the SNR is increased. Figure 13 shows the normalized thresholds $U/\sqrt{E_b}$ yielding the minimum BER for the different number of retransmissions D. Finally, Figure 14 shows the BER versus the SNR γ_b for the different number of retransmissions D assuming the optimum thresholds $U/\sqrt{E_b}$ for each SNR that achieves the minimum BER. The minimization of BER by optimizing the threshold $U/\sqrt{E_b}$ is again more effective when the SNR is increased. The performance of this bitwise retransmission scheme with $D \geq 1$ and rate $R_f > 1/2$ is at least 3 dB better than that of the rate $1/2$ BRC in exchange of larger implementation complexity.

4.4. Feedback signaling

There are two main issues when designing practical schemes involving feedback signaling. The first issue is how to constrain the number of feedback bits. The second issue is feedback bits errors.

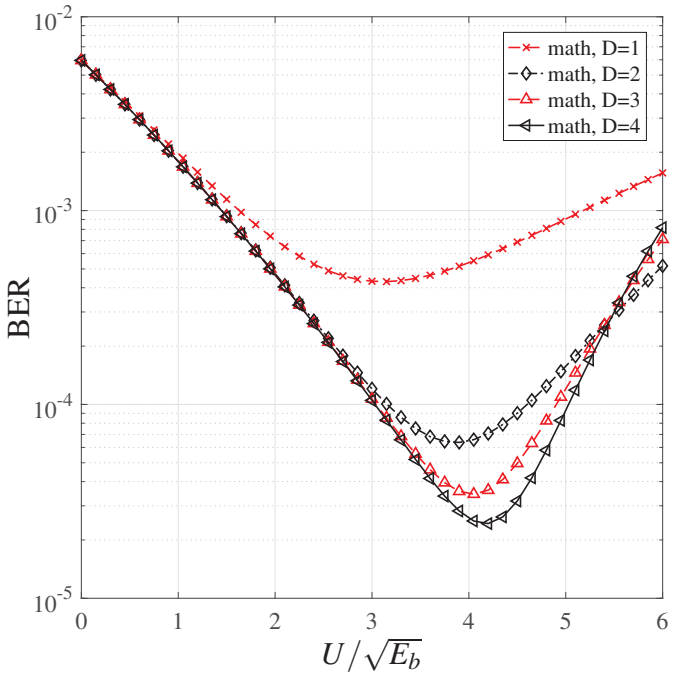

Figure 12: The BER versus the normalized threshold $U/\sqrt{E_b}$ for the SNR $\gamma_b = 5$ dB and the different number of retransmissions D.

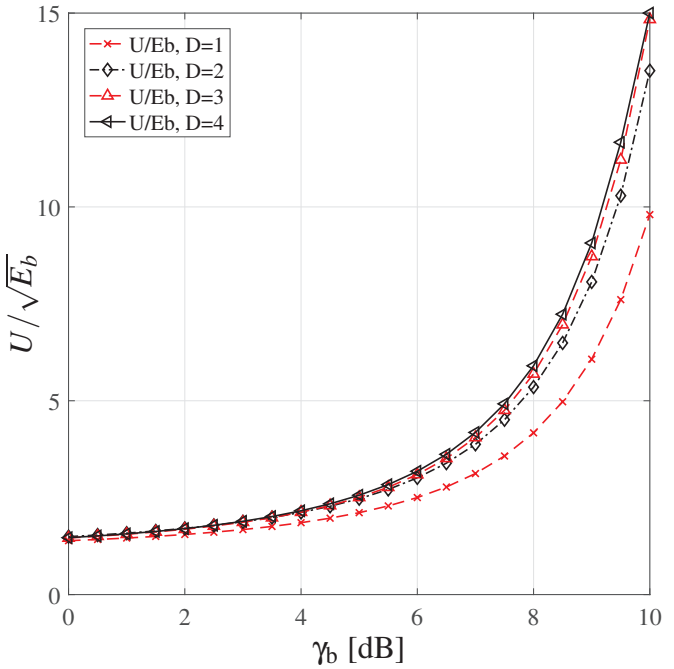

Figure 13: The values of the normalized threshold $U/\sqrt{E_b}$ corresponding to the minimum BER versus the SNR γ_b for the different number of retransmissions D.

Sending only a small number of feedback bits in a dedicated packet is very inefficient due to the associated overhead. In practice, it is common to reserve a few bits within the packet payload for feedback signaling, so the protocol overhead is shared by the feedback as well as data bits. In such

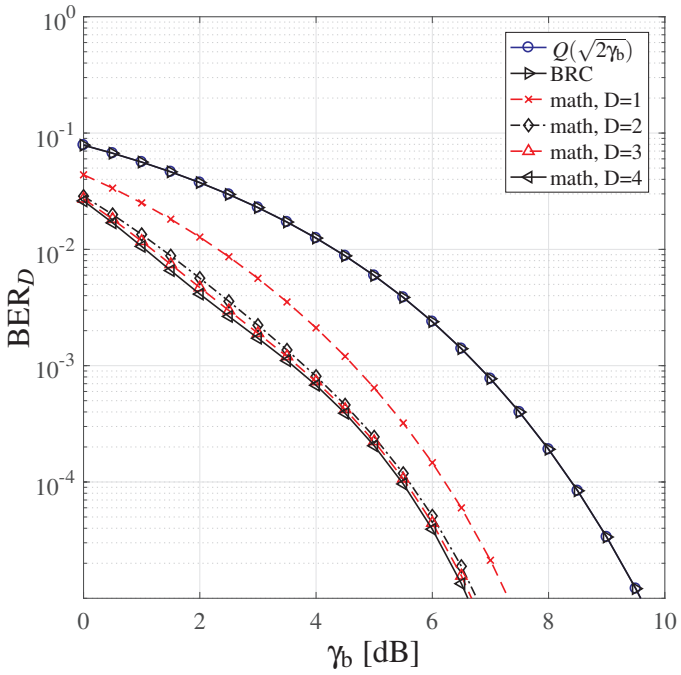

Figure 14: The BER_D versus the SNR γ_b for the different number of retransmissions D.

case, it is beneficial to minimize the number of feedback bits and increase the data payload. We can reduce the number of feedback bits sent from the destination to the source over a reverse link by considering a deterministic sequence of bit permutations synchronously generated at the transmitter and at the receiver to encode the feedback message. The permutations are conveniently generated as a pseudo-random sequence of N-tuples, $(1,2,\ldots,N)$, using two synchronized random number generators (RNGs) at the transmitter and at the receiver, respectively. Both RNGs are configured to synchronously advance by exactly 2^{C_1} permutations during each symbol period where C_1 is an integer. For every generated permutation, the receiver checks whether a sufficient number of permuted received bits with small reliability fall into a predefined window of W bits. For instance, we can assume that the retransmission window is represented by the the first W bit positions in the packet. When such permutation is found, the feedback message to notify the source is a binary representation of the permutation number modulo 2^{C_1}. The source then selects the corresponding W bits in the packet, and retransmits them to the destination. For the given window size W, the number of permutations K searched until the desired one has been found can be expressed as,

$$K = 2^{C_1} I + (K \bmod 2^{C_1})$$

where I is an integer number of the idle symbol periods. The key property is that,

$$(K \bmod 2^{C_1}) \ll \binom{N}{W}$$

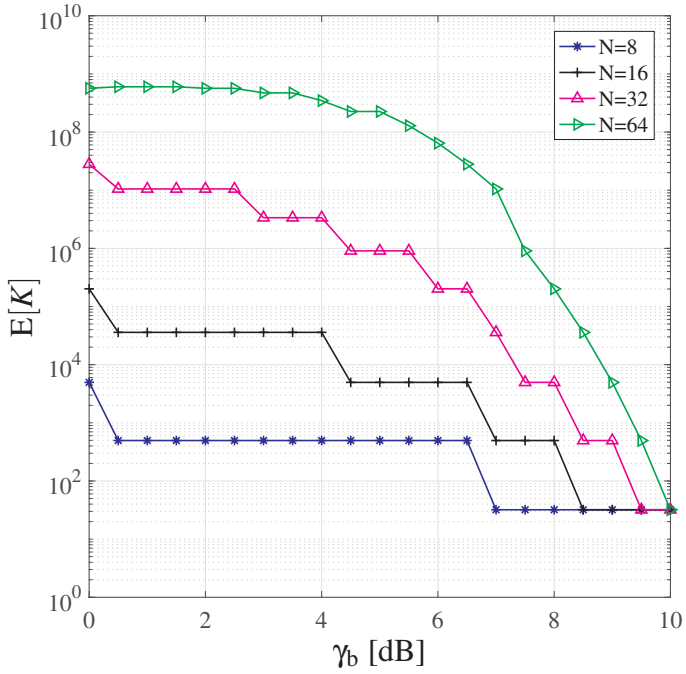

Figure 15: The expected number of permutations E[K] versus the SNR γ_b and the different packet length N.

whereas, on average, $\mathrm{E}[K] = \binom{N}{W}$ where $\binom{N}{W}$ denotes the binomial number. Hence, the feedback message is only represented by C_1 bits. The value of C_1 is a design parameter and trade-offs the feedback message size with the required delay until the start of the next retransmission [23].

More importantly, given the target BER, the window size W and the average number of searched permutations E[K] are decreasing with SNR. As shown in Figure 15, E[K] is only about 30 for the packet length $N \leq 64$ and the SNR at least 10 dB; then, the feedback of $C_1 = 5$ bits can be used to find the desired permutation during only one symbol period.

The average forward throughput with one retransmission can be defined as,

$$\zeta_1 = \frac{N}{\mathrm{E}[I+1]}.$$

By simulations, we found that there exists an optimum value C_1^* which minimizes the expected delay E[$I+1$], i.e., which maximizes the throughput ζ_1. This optimum value is given as,

$$C_1^* = \lceil -0.5 + \log_2 \mathrm{E}[K] \rfloor$$

and it is plotted in Figure 16 for different values of packet lengths N. The corresponding maximum throughput ζ_1^* is shown in Figure 17. For comparison, the throughput of the BRC with one retransmission is also shown in Figure 17. We observe that our bitwise retransmission scheme generally achieves a better throughput than the rate $1/D$ BRC for the same number of retransmissions D, especially at the medium to large values of SNR. Furthermore, we can show that the throughput of

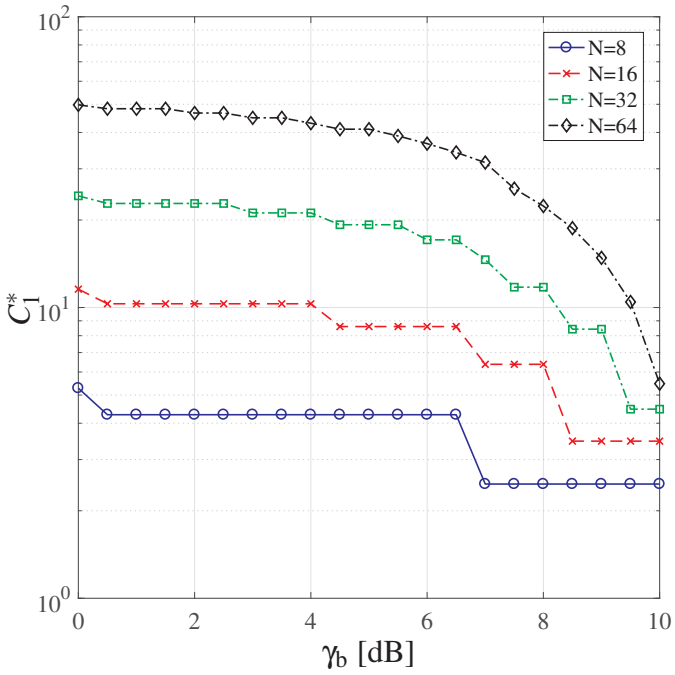

Figure 16: The optimum values C_1^* with $D = 1$ retransmission versus the SNR γ_b for the different packet length N.

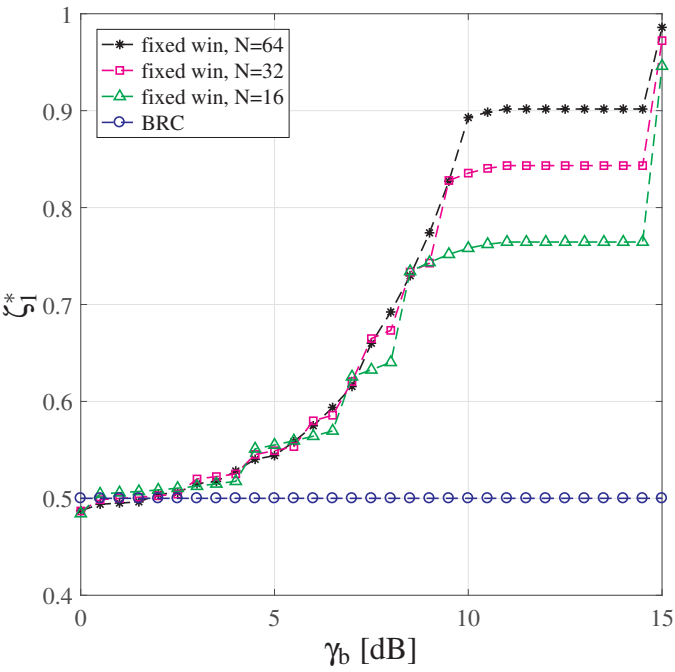

Figure 17: The throughput ζ_1^* corresponding to the optimum values C_1^* versus the SNR γ_b for the different packet length N.

the fixed window technique in the limit of very large SNR converges to, $\lim_{\gamma_b \to \infty} \zeta_1 \approx \frac{N}{N+1}$, since $\lim_{\gamma_b \to \infty} W/N = 0$.

Finally, we reconsider the assumption of the error-free feedback which is often adopted in literature concerning ARQ retransmissions. In particular, it was shown in [11] that errors of 1 or 2-bit

feedback messages can be neglected if the corresponding bit error probability is less than 10^{-3}. This result can be readily modified for our case of multi-bit feedback utilized in the bitwise retransmission schemes. Thus, assuming that the feedback bit errors are independent, and they occur with the probability p_r, we have the following proposition.

Proposition 4. *The bit errors in the feedback message of C bits can be tolerated, provided that their bit-error probability is bounded as,*

$$p_r \leq 1 - P_{\min}^{1/C}$$

where the required minimum probability of the error-free feedback message was established in [11] to be, $P_{\min} = 1 - 10^{-3} = 99.9\%$.

The proof of Proposition 4 follows from the binomial distribution of independent and equally probable errors. Proposition 4 shows that the longer the feedback message, the smaller the feedback bit error probability p_r is required.

5. BER Performance in Fading Channels

Referring to the BER analysis in Section 3, we numerically compare the performance of the bitwise retransmission schemes over AWGN and slow (block) and fast fading channels. For all retransmission schemes considered, the SNR $\gamma_{\rm b}$ is normalized by the forward rate $R_{\rm f}$, so the smaller W, the larger $R_{\rm f}$ and the larger SNR is set in simulations. Note also that, in general, the bitwise retransmission schemes assume $0 < W \ll N$ whilst the cases, $W = 0$ and $W = N$, correspond to the conventional retransmission schemes.

Consider first the case of uncoded transmissions of packets of N binary modulation symbols. For simplicity, we assume one retransmission of exactly W least reliable bits. The simulation results for the packets of $N = 128$ bits, and $W = 1$, 2, 4 and 8 retransmitted bits over the AWGN channel, and $W = 8$ and $W = 128$ retransmitted bits over the slow fading channel, respectively, are shown in Figure 18. Note that the rate $1/2$ BRC represents a stop-and-wait ARQ scheme with one retransmission of the whole packet. As discussed in the previous section, for the AWGN channel (or, equivalently, for a very slowly fading channel), there exists an optimum number of retransmitted bits to minimize the BER. For instance, when $W = N = 128$, we have a rate $1/2$ BRC whose BER performance coincides with the BER of binary antipodal signaling given by $Q(\sqrt{2\gamma_{\rm b}})$ whereas 3.5 dB gain in SNR over $1/2$ BRC can be obtained for the retransmission window size of $W = 8$ bits. However, for slow fading channels where the SNR of the initial received packet and the SNR of the retransmitted W bits

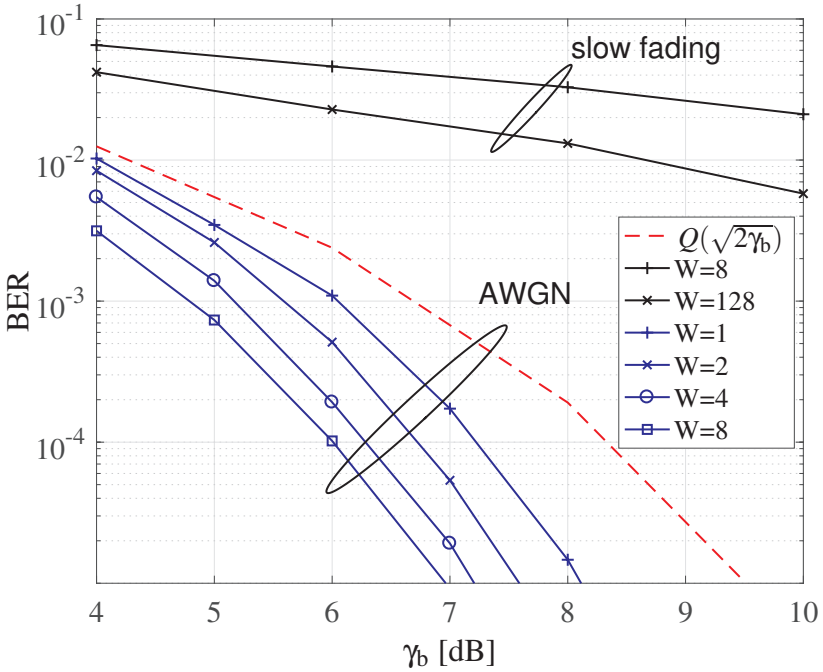

Figure 18: The BER versus SNR γ_b for an uncoded ARQ with $D = 1$ bitwise retransmission of the W least reliable bits over AWGN and slow fading channels.

are independent, the BER performance monotonically increases with W, so the rate $1/2$ BRC always outperforms other bitwise retransmission schemes with $W < N$.

The BER results for a fast fading channel with independent SNR of each received binary symbol are shown in Figure 19. We observe that the scheme with $W = 2$ retransmitted bits is within 1.5 dB from the rate $1/2$ BRC corresponding to $W = 128$ bits whereas the new scheme has the gain of about 10 dB over the case with no retransmissions. The smaller values W provide the second order diversity for the smaller number of bits which increases the BER. In general, by selecting the W least reliable bits, the bitwise retransmission scheme implements the W out of N selection diversity.

5.1. The FEC coded bitwise retransmissions

As an example of the HARQ scheme with FEC coding, we consider a rate $R = 1/3$ convolutional code (CC) having the generating polynomials 13, 15 and 17 (in octal notation), the constraint length 4, and the minimum free Hamming distance $d_{\text{free}} = 10$ [24, p. 178]. The soft-decision decoding corresponding to the maximum-likelihood (ML) sequence decoding is implemented by the Viterbi algorithm. The number of input information bits is set to $N = 128$, so the number of output encoded bits is $128 \times 3 = 384$.

The FEC coded HARQ signaling sends at first a punctured rate $1/2$ codeword of $128 \times 2 = 256$ bits created by removing all parity bits of one of the three polynomial generators. If the punctured code-

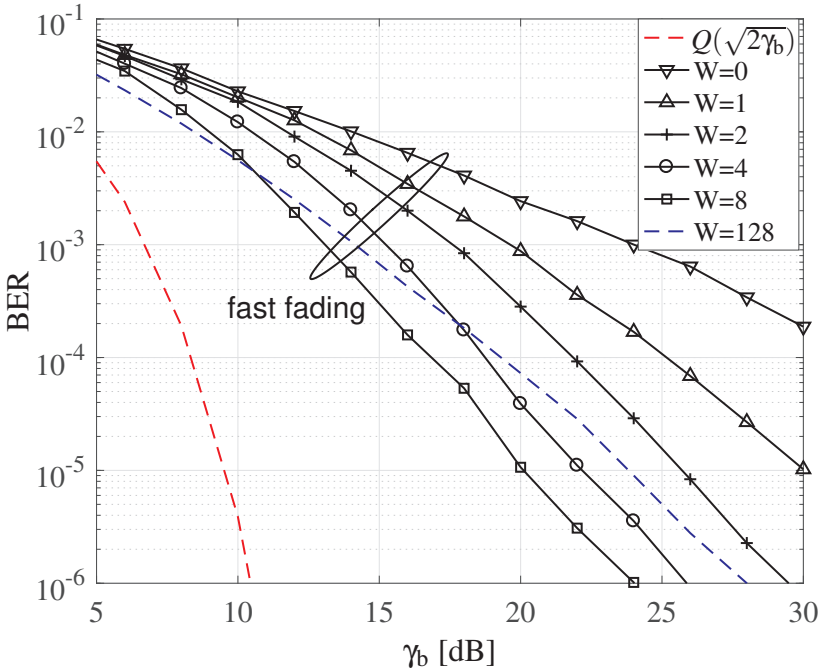

Figure 19: The BER versus SNR γ_b for an uncoded ARQ with $D = 1$ bitwise retransmission of the W least reliable bits over a fast fading channel.

word cannot be decoded correctly, the decoder requests the additional IR represented by the removed 128 bits in the encoder. The BER performance of this conventional HARQ scheme is compared with the following bitwise retransmission scheme. As before, the rate $1/2$ punctured CC codeword of 256 bits is sent first. However, now, instead of sending the punctured 128 parity bits as in the case of conventional HARQ, the encoder re-sends only a small number of W least reliable bits which were received previously. Figure 20 shows that, in a AWGN channel, resending only $W = 1$ bit can bring the BER performance to be within 1 dB from the full rate $1/3$ CC. Moreover, the BER performance of the punctured rate $1/2$ CC with no additional IR denoted as $W = 0$ is improved by 2.5 dB, if only $W = 1$ bit of the IR is used. In a slow fading channel, the gain of the punctured $1/2$ CC with $W = 1$ bit of the IR is about 3 dB compared to the case with no additional IR.

The results for the CC transmissions over fast fading channel are shown in Figure 21. In this case, the selection diversity of the bitwise retransmission scheme with $W = 8$ bits of IR can even outperform the full rate $1/3$ CC for the SNRs above 8.5 dB; however, it under-performs the full rate $1/3$ CC by about 1 dB when the IR is only $W = 2$ bits. The number of feedback bits for these two bitwise retransmission schemes are, $C = \lceil \log_2 \binom{128}{8} \rceil = 41$ bits and $C = \lceil \log_2 \binom{128}{2} \rceil = 13$ bits, respectively.

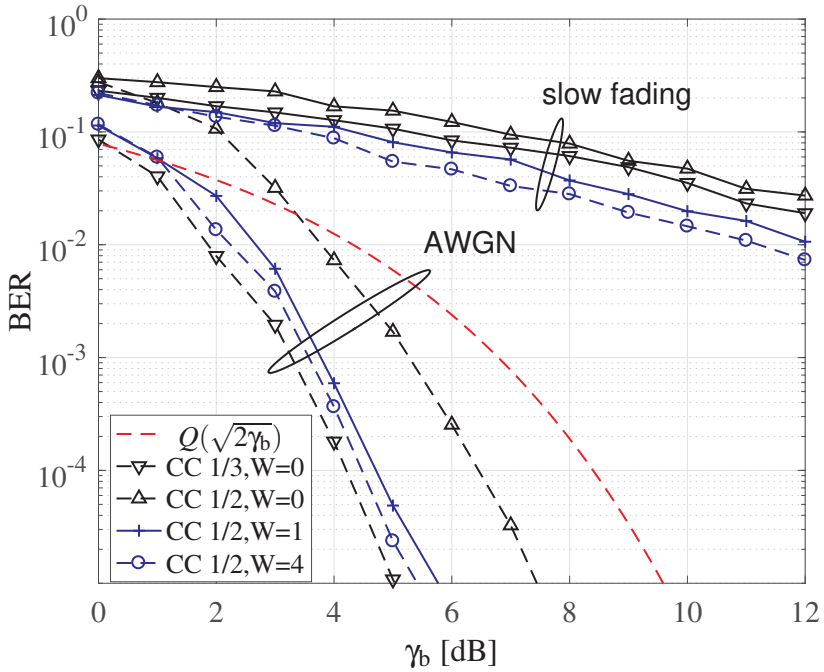

Figure 20: The BER versus SNR γ_b for a HARQ scheme employing the rate $1/3$ ($1/2$ after puncturing) CC and a single IR retransmission containing W least reliable bits over AWGN and slow fading channels.

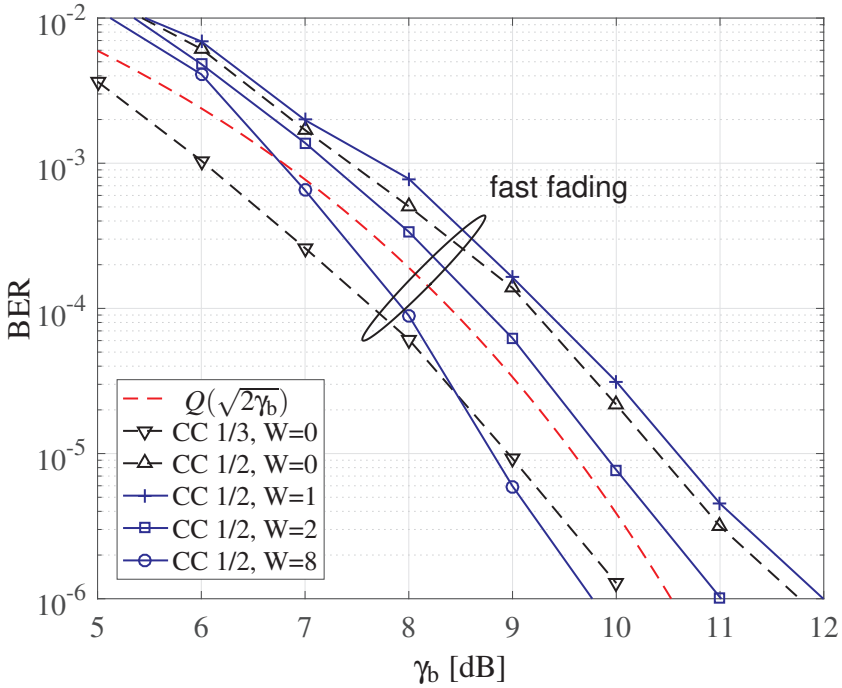

Figure 21: The BER versus SNR γ_b for a HARQ scheme employing the rate $1/3$ ($1/2$ after puncturing) CC and a single IR retransmission containing W least reliable bits over a fast fading channel.

6. Data Fusion Application

We now illustrate the use of bitwise retransmission schemes to improve the reliability of data fusion from a group of L sensor nodes connected to a single central access point (AP). A time-division

multiple access (TDMA) protocol with $(L+1)$ time slots is used to share the communication channel. The time-division duplex (TDD) assigns the time slots into L uplink time slots to transmit the data from L sensor nodes, and one time slot is allocated for feedback signaling from the AP. Each time slot can carry at most N bits of information including the protocol overhead. The AP is assumed not to be battery powered, so the transmit power in the downlink can be much larger than in the battery and computing constrained uplink.

More specifically, we consider the following three sensor node technologies: Zigbee 802.15.4, WiFi 802.11b and Bluetooth v. 4.2 802.15.1. The parameters of these three technologies are summarized in Table 1. Their BER performances have been obtained by fitting the sum of exponentials (the Prony method, [26]) to the BER curves reported in [27]. From Table 1, it is obvious that Zigbee is the most energy efficient technology for the sensor nodes, and it can also operate at small SNR values.

The specific design examples of the bitwise retransmission schemes with a constant retransmission window size employing the binomial number feedback and the packet segmentation are listed in Table 2. Therein, p_f is the BER of the forward link, p_r is the BER of the reverse link, N_{seg} is the number of equal-length segments partitioning the N bit packet, W_{seg} is the retransmission window size per segment, and C_{tot} is the total length of the feedback message (in bits) required for the whole packet. Hence, N/N_{seg} is the segment length, $W_{\text{seg}}N_{\text{seg}} = W$ is the total number of retransmitted bits, and $C_{\text{tot}}/N_{\text{seg}}$ is the size of the feedback message per segment. Assuming independent transmission bit errors, $\tilde{P}_f$ denotes the probability (calculated using a binomial distribution) that there are at most W_{seg} errors in any segment (i.e., the closer the value of $\tilde{P}_f$ to 1.0, the better), and $\tilde{P}_r$ is the probability (calculated using a binomial distribution) that there is at least one bit error among the C_{tot} feedback bits received at the source (i.e., the probability that the feedback message is received incorrectly at the source). As shown in the previous section, it is required that $\tilde{P}_r < P_{\min} = 10^{-3}$ in order to be able to neglect the effect of feedback bit errors on the BER performance. Other system parameters are given in Table 1 including the packet size N and the required SNRs for the given values of p_f.

In order to design practical bitwise retransmission schemes, we found that the BER p_f of the forward link should be at most 10^{-3}, and the BER p_r of the reverse link should be at most 10^{-5}. In terms of the minimum required SNR for bidirectional communications, these BERs translate to -1.16 dB and 0.96 dB for the Zigbee, 5.43 dB and 7.59 dB for the WiFi, and 10.93 dB and 13.34 dB for the Bluetooth in the uplink and in the downlink, respectively. Such SNR levels can be satisfied for all three wireless technologies considered, provided that the reverse link (downlink) has only 3 dB larger transmission power than the forward link (uplink). Such transmission power unbalances can be read-

Table 1: The transmission parameters of the three sensor node technologies

	Zigbee	WiFi	Bluetooth
BER	$P_b(\gamma_b) = 1.5203\,e^{-9.5611\gamma_b}$	$P_b(\gamma_b) = 10.0\,e^{-3.4535\gamma_b} + 1.1066\,e^{-2.0247\gamma_b}$	$P_b(\gamma_b) = 0.2436\,e^{-0.4997\gamma_b} + 0.2436\,e^{-0.4997\gamma_b}$
	γ_b [dB]	γ_b [dB]	γ_b [dB]
10^{-2}	-2.79	3.88	8.91
10^{-3}	-1.16	5.43	10.93
10^{-4}	0.03	6.63	12.30
10^{-5}	0.96	7.59	13.34
10^{-6}	1.73	8.37	14.18
Packet	header	preamble+header	header+CRC
[bytes]	6	15–24	2+2
	payload	payload	payload
	127	1500	252
N [bits]	$(6+127)\times 8 = 1064$	$(24+1500)\times 8 = 12192$	$(4+252)\times 8 = 2048$
Segments	14×76, 19×56, 28×38 38×28, 56×19, 76×14 133×8, 152×7, 266×4 532×2, 1064×1	16×762, 32×381, 48×254 96×127, 127×96, 254×48 381×32, 508×24, 762×16 1016×12, 1524×8, 2032×6 3048×4, 4064×3, 6096×2 12192×1	16×128, 32×64, 64×32 128×16, 256×8, 512×4 1024×2, 2048×1

ily obtained in the sensor networks with the centralized mains-powered AP. The AP has also sufficient computing resources to determine the W least reliable bits to be requested for retransmission.

Next, we consider scheduling of data and feedback bits within the packets for our single-cell TDMA/TDD multiple access protocol. We assume that the parameters W, D, N, L and C_{tot} are constant, even though they can be optimized for the required uplink and downlink BERs p_f and p_r, respectively. Recall that all packets have the maximum length of N bits. In the uplink, the nodes send their current data as well as schedule the retransmitted bits for the previously transmitted packets. In the downlink, the AP broadcasts the retransmission requests to all sensor nodes at once. The bits in the uplink packets are scheduled following these two rules.

1. Insert first the retransmitted sequences in the order corresponding to the previously transmitted

packets. Only one retransmitted sequence per each previously transmitted packet is scheduled.

2. Add data bits from the buffered information blocks which have not yet been transmitted to fill the remaining bit positions in the packet.

Hence, the transmitted packets can contain retransmitted bits for several previously transmitted packets, and also data bits from multiple information blocks. As an example, assuming the first-in first-out (FIFO) buffering of information blocks of $N_{\text{buf}} = N = 1064$ bits (Zigbee protocol) with $N_{\text{seg}} = 2$ segments, $W_{\text{seg}} = 2$ retransmitted bits, i.e., the total retransmission window size of $W = 2 \times 2 = 4$ bits, $D = 3$ retransmissions, and in total, $L_{\text{pac}} = 10$ packets of information blocks to be transmitted, the packet contents schedule is shown in Table 3. Therein, we use the notation $\mathrm{D}_l(n)$ to denote a sequence of n bits belonging to the l-th information block, and $\mathrm{R}_{l,d}(m)$ is the sequence of m retransmitted bits in the d-th retransmission for the l-th information block where the sequence indexes, $1 \leq l \leq L_{\text{pac}}$, $1 \leq n \leq N$, $1 \leq d \leq D$ and $1 \leq m \leq W$. We have the following proposition.

Proposition 5. *For given $N \gg DW$, $N_{\text{buf}} = N$ and $L_{\text{pac}} \geq 1$, only the very first information block is completely transmitted in the first packet whereas all other information blocks are split into exactly 2 subsequent packets. The D retransmissions are scheduled into D subsequent packets immediately after the initial transmission of the corresponding information block was completed. Moreover, only the first L_{pac} transmitted packets are fully occupied with N bits. The available transport capacity in the subsequent last $(D+1)$ transmitted packets can be used to transmit new information blocks with the progressively longer bit segments to fill N bit packets.*

The key assumption required in Proposition 5 is that the total number of retransmitted bits $D \cdot W$ is much smaller than the block length N. If this condition is not satisfied, the packet structure of the bitwise retransmission scheme is less predictable.

Table 2: The bitwise retransmission designs with the constant window size and the packet segmentation

	p_f	p_r	N_{seg}	W_{seg}	C_{tot}	$\tilde{P}_f$	$\tilde{P}_r$
Zigbee	10^{-3}	10^{-5}	2	3	50	0.9978	$5.0 \cdot 10^{-4}$
	10^{-3}	10^{-5}	1	4	36	0.9953	$3.6 \cdot 10^{-4}$
	10^{-3}	10^{-5}	1	5	44	0.9992	$4.4 \cdot 10^{-4}$
	10^{-4}	10^{-5}	4	1	36	0.9997	$3.6 \cdot 10^{-4}$
	10^{-4}	10^{-5}	2	1	20	0.9986	$2.0 \cdot 10^{-4}$
	10^{-4}	10^{-5}	2	2	36	1.0000	$3.6 \cdot 10^{-4}$
	10^{-4}	10^{-5}	2	3	50	1.0000	$5.0 \cdot 10^{-4}$
	10^{-4}	10^{-5}	1	1	11	0.9947	$1.1 \cdot 10^{-4}$
	10^{-4}	10^{-5}	1	2	20	0.9998	$2.0 \cdot 10^{-4}$
	10^{-4}	10^{-5}	1	3	28	1.0000	$2.8 \cdot 10^{-4}$
	10^{-4}	10^{-5}	1	4	36	1.0000	$3.6 \cdot 10^{-4}$
WiFi	10^{-3}	10^{-6}	1	21	220	0.9928	$2.2 \cdot 10^{-4}$
	10^{-4}	10^{-6}	4	2	92	0.9962	$9.2 \cdot 10^{-5}$
	10^{-4}	10^{-6}	3	2	69	0.9917	$6.9 \cdot 10^{-5}$
	10^{-4}	10^{-6}	2	3	72	0.9965	$7.2 \cdot 10^{-5}$
	10^{-4}	10^{-6}	2	4	92	0.9996	$9.2 \cdot 10^{-5}$
	10^{-4}	10^{-6}	1	4	50	0.9917	$5.0 \cdot 10^{-5}$
	10^{-4}	10^{-6}	1	5	61	0.9984	$6.1 \cdot 10^{-5}$
	10^{-4}	10^{-6}	1	6	72	0.9997	$7.2 \cdot 10^{-5}$
	10^{-4}	10^{-6}	1	7	83	1.0000	$8.3 \cdot 10^{-5}$
	10^{-4}	10^{-6}	1	8	94	1.0000	$9.4 \cdot 10^{-5}$
Bluetooth	10^{-2}	10^{-6}	2	18	256	0.9913	$2.6 \cdot 10^{-4}$
	10^{-3}	10^{-6}	2	4	72	0.9960	$7.2 \cdot 10^{-5}$
	10^{-3}	10^{-6}	1	6	57	0.9949	$5.7 \cdot 10^{-5}$
	10^{-3}	10^{-6}	1	7	65	0.9987	$6.5 \cdot 10^{-5}$
	10^{-3}	10^{-6}	1	8	73	0.9997	$7.3 \cdot 10^{-5}$
	10^{-4}	10^{-5}	4	1	36	0.9987	$3.6 \cdot 10^{-4}$
	10^{-4}	10^{-5}	2	1	20	0.9951	$2.0 \cdot 10^{-4}$
	10^{-4}	10^{-5}	2	2	38	0.9998	$3.8 \cdot 10^{-4}$
	10^{-4}	10^{-5}	1	2	21	0.9988	$2.1 \cdot 10^{-4}$
	10^{-4}	10^{-5}	1	3	31	0.9999	$3.1 \cdot 10^{-4}$
	10^{-4}	10^{-5}	1	4	40	1.0000	$4.0 \cdot 10^{-4}$

Table 3: The uplink packet contents for $N = 1064$, $W = 4$, $D = 3$, $L_{\text{pac}} = 10$

#	packet content
1	$D_1(1064)$
2	$R_{1,1}(4)$, $D_2(1060)$
3	$R_{1,2}(4)$, $D_2(4)$, $D_3(1056)$
4	$R_{1,3}(4)$, $R_{2,1}(4)$, $D_3(8)$, $D_4(1048)$
5	$R_{2,2}(4)$, $R_{3,1}(4)$, $D_4(16)$, $D_5(1040)$
6	$R_{2,3}(4)$, $R_{3,2}(4)$, $R_{4,1}(4)$, $D_5(24)$, $D_6(1028)$
7	$R_{3,3}(4)$, $R_{4,2}(4)$, $R_{5,1}(4)$, $D_6(36)$, $D_7(1016)$
8	$R_{4,3}(4)$, $R_{5,2}(4)$, $R_{6,1}(4)$, $D_7(48)$, $D_8(1004)$
9	$R_{5,3}(4)$, $R_{6,2}(4)$, $R_{7,1}(4)$, $D_8(60)$, $D_9(992)$
10	$R_{6,3}(4)$, $R_{7,2}(4)$, $R_{8,1}(4)$, $D_9(72)$, $D_{10}(980)$
11	$R_{7,3}(4)$, $R_{8,2}(4)$, $R_{9,1}(4)$, $D_{10}(84)$
12	$R_{8,3}(4)$, $R_{9,2}(4)$, $R_{10,1}(4)$
13	$R_{9,3}(4)$, $R_{10,2}(4)$
14	$R_{10,3}(4)$

In addition to the uplink packet structure, we need to specify the packet structure also in the downlink. According to Proposition 5, the AP (the data fusion center) sends the retransmission requests for the l-th information block during the time slots $\{1,2,\ldots,D\}$, if $l = 1$, and $\{l+1, l+2, \ldots, l+D\}$, for $l \geq 2$. However, since the information blocks with the index $l \geq 2$ are transmitted exactly in two subsequent packets with the indexes l and $l+1$, the number of retransmission requests contained in the downlink packet first raises to the maximum value of D requests per sensor node. The number of the requests then remain constant until it is gradually decremented to only 1 request in the last $(D-1)$ downlink transmissions. Consequently, we have the following proposition.

Proposition 6. *The maximum number of sensor nodes $L_{\max}$ which can be supported by the retransmission scheme described in this section is bounded as,*

$$L_{\max} \leq \left\lceil \frac{N - N_{\text{ovh}}}{D \cdot C_{\text{tot}}} \right\rceil$$

where N_{ovh} is the protocol overhead, and C_{tot} is the total number of feedback bits per retransmission and sensor node.

Continuing the example in Table 3, and assuming $N_{\text{ovh}} = 106$ bits of protocol overhead (10% of the

packet length N), we have that $C_{\text{tot}} = 36$ bits, so $L_{\max} \leq 8$. A larger number of sensor nodes could be supported by trading-off the number of feedback bits C_{tot} with the number of retransmissions. In addition, it is possible as well as likely that different sensor nodes set their retransmission parameters differently, for example, to match their connection link quality. In this case, the value of $L_{\max}$ in Proposition 6 can be calculated by assuming the maximum total number of feedback bits, $\max_l(D \cdot C_{\text{tot}})$, allowed per any sensor node $l = 1, \ldots, L$.

7. Conclusion

The previously proposed bitwise retransmission scheme was analyzed to selectively retransmit only the bits which are received with small reliability. The bitwise retransmission decisions and combining of the received bits can be done either immediately after demodulation of received symbols, or after the channel decoding. The lower implementation complexity of the bitwise retransmission schemes relative to HARQ and pure FEC coding is exchanged for a larger number of feedback bits.

Mathematical analysis of bitwise retransmission schemes was performed assuming uncoded binary modulation over an AWGN channel. It was shown that the bitwise retransmissions can be optimized for given system parameters including SNR. In addition to minimizing the BER as investigated in this paper, it is possible to instead maximize the throughput. The computationally efficient and accurate approximations of the BER were verified by computer simulations. We also specified the conditions when the effect of feedback errors on the overall performance can be neglected.

The BER performance of three specific bitwise retransmission policies were evaluated. They are referred to as the fixed rate technique, the fixed window technique, and the fixed threshold technique. These schemes always outperform the traditional repetition diversity over AWGN channels. Furthermore, the BER performance of the uncoded and coded bitwise retransmissions were compared over AWGN, slow fading and fast fading channels. We found that the bitwise retransmissions are beneficial when the link SNR is either constant during all retransmissions which occur for very slowly fading channels with the minimum mobility as well as when the link SNR changes independently from between the received symbols. In such fast fading channels, the bitwise retransmissions benefit from the selection diversity, and can even outperform the conventional HARQ at large SNRs.

Finally, we designed a retransmission protocol for data collection in wireless sensor networks with a single data fusion center. Assuming the actual parameters of Zigbee, WiFi and Bluetooth, the scheduling of data bits, retransmitted bits, and the retransmission request bits was specified for the uplink and downlink packets, respectively, so that all transmitted packets are fully occupied. The

smaller BER required for transmitting the feedback bits in the downlink can be readily achieved by increasing the transmission power of the central AP.

Appendix

We present approximations to efficiently evaluate the probabilities and the BER expressions obtained in Section 3. These approximations are verified numerically in Section 4. They are based on the so-called Prony approximation of the $Q(x)$ function [26], i.e.,

$$Q(x) = \sum_{k=1}^{2} A_k \, \mathrm{e}^{-B_k x^2}$$

where $A_1 = 0.208$, $A_2 = 0.147$, $B_1 = 0.971$, and $B_2 = 0.525$, and $\mathrm{erf}(x) = 1 - 2Q\left(\sqrt{2}x\right)$. The sign function is denoted as $\mathrm{sign}(\cdot)$.

Integral approximations

Assuming positive constants $H > 0$, and $h_i > 0$, $i = 1,2,3,4,5$, we have the following integral approximations,

$$\int_{-\infty}^{0} h_1 \, \mathrm{e}^{-\frac{(\bar{r}-h_2)^2}{h_3}} Q(h_4(h_5-\bar{r})) \, \mathrm{d}\bar{r} \approx$$
$$\sum_{k=1}^{2} \int_{-\infty}^{0} h_1 \, \mathrm{e}^{-\frac{(\bar{r}-h_2)^2}{h_3}} A_k \, \mathrm{e}^{-B_k(h_4(h_5-\bar{r}))^2} \, \mathrm{d}\bar{r} \approx \sum_{k=1}^{2} \frac{h_1 A_k \sqrt{\pi}}{2\sqrt{\frac{1}{h_3}+{h_4}^2 B_k}} \, \mathrm{e}^{-\frac{B_k {h_4}^2 (h_2-h_5)^2}{1+h_3 {h_4}^2 B_k}} \, \mathrm{erfc}\left(\frac{h_2+h_3 {h_4}^2 h_5 B_k}{\sqrt{h_3(1+h_3 {h_4}^2 B_k)}} \right)$$

$$\int_{-\infty}^{0} h_1 \, \mathrm{e}^{-\frac{(\bar{r}-h_2)^2}{h_3}} Q(h_4(h_5+\bar{r})) \, \mathrm{d}\bar{r} \approx$$
$$\sum_{k=1}^{2} \int_{-\infty}^{0} h_1 \, \mathrm{e}^{-\frac{(\bar{r}-h_2)^2}{h_3}} A_k \, \mathrm{e}^{-B_k(h_4(h_5+\bar{r}))^2} \, \mathrm{d}\bar{r} \approx \sum_{k=1}^{2} \frac{h_1 h_3 A_k \sqrt{\pi}}{2\sqrt{h_3(1+h_3 {h_4}^2 B_k)}} \, \mathrm{e}^{-\frac{B_k {h_4}^2 (h_2+h_5)^2}{1+h_3 {h_4}^2 B_k}} \, \mathrm{erfc}\left(\frac{h_2-h_3 {h_4}^2 h_5 B_k}{\sqrt{h_3(1+h_3 {h_4}^2 B_k)}} \right)$$

$$\int_{-H}^{H} h_1 \, \mathrm{e}^{-\frac{(\bar{r}-h_2)^2}{h_3}} Q(h_4(h_5-\bar{r})) \, \mathrm{d}\bar{r} \approx$$
$$\sum_{k=1}^{2} \int_{-H}^{H} h_1 \, \mathrm{e}^{-\frac{(\bar{r}-h_2)^2}{h_3}} A_k \, \mathrm{e}^{-B_k(h_4(h_5-\bar{r}))^2} \, \mathrm{d}\bar{r} \approx \sum_{k=1}^{2} \frac{h_1 A_k \sqrt{h_3}\sqrt{\pi}}{2\sqrt{1+h_3 {h_4}^2 B_k}} \, \mathrm{e}^{-\frac{B_k {h_4}^2 (h_2-h_5)^2}{1+h_3 {h_4}^2 B_k}} \times$$
$$\left\{ \mathrm{erf}\left(\frac{h_2+H+h_3 {h_4}^2 (h_5+H) B_k}{\sqrt{h_3(1+h_3 {h_4}^2 B_k)}} \right) + \mathrm{sign}\left(H - \frac{h_2+h_3 {h_4}^2 h_5 B_k}{1+h_3 {h_4}^2 B_k} \right) \mathrm{erf}\left(\sqrt{\frac{1}{h_3}+{h_4}^2 B_k} \left| H - \frac{h_2+h_3 {h_4}^2 h_5 B_k}{1+h_3 {h_4}^2 B_k} \right| \right) \right\}$$

$$\int_{-H}^{H} h_1 \, \mathrm{e}^{-\frac{(\bar{r}-h_2)^2}{h_3}} Q(h_4(h_5+\bar{r})) \, \mathrm{d}\bar{r} \approx$$
$$\sum_{k=1}^{2} \int_{-H}^{H} h_1 \, \mathrm{e}^{-\frac{(\bar{r}-h_2)^2}{h_3}} A_k \, \mathrm{e}^{-B_k(h_4(h_5+\bar{r}))^2} \, \mathrm{d}\bar{r} \approx \sum_{k=1}^{2} \frac{h_1 h_3 A_k \sqrt{\pi}}{2\sqrt{h_3(1+h_3 {h_4}^2 B_k)}} \, \mathrm{e}^{-\frac{B_k {h_4}^2 (h_2+h_5)^2}{1+h_3 {h_4}^2 B_k}} \times$$
$$\left\{ \mathrm{erf}\left(\frac{H+h_2+h_3 {h_4}^2 (H-h_5) B_k}{\sqrt{h_3(1+h_3 {h_4}^2 B_k)}} \right) + \mathrm{erf}\left(\frac{H-h_2+h_3 {h_4}^2 (H+h_5) B_k}{\sqrt{h_3(1+h_3 {h_4}^2 B_k)}} \right) \right\}$$

BER approximation in Section 3.1

The BER_1 can be accurately approximated as,

$$\begin{aligned}\mathrm{BER}_1 \;\approx\; & Q\Big(\sqrt{2\gamma_\mathrm{b}}(\frac{U_0}{2\gamma_\mathrm{b}}+1)\Big)+Q\Big(\sqrt{4\gamma_\mathrm{b}}\Big)-\sum_{k=1}^{2}\frac{A_k}{\sqrt{1+2B_k}}\times \\ & \times\Big\{\mathrm{e}^{-\alpha_{k,1}^{-}(U_0)\gamma_\mathrm{b}}Q\Big(\beta_{k,1}^{+}(U_0)\sqrt{\gamma_\mathrm{b}}\Big)+\mathrm{e}^{-\alpha_{k,1}^{+}(U_0)\gamma_\mathrm{b}}Q\Big(\beta_{k,1}^{-}(U_0)\sqrt{\gamma_\mathrm{b}}\Big)\Big\}\end{aligned}$$

where the coefficients A_k and B_k are defined above, and the auxiliary functions,

$$\alpha_{k,d}^{-}(U)=\frac{B_k(d+1)(2-U/\gamma_\mathrm{b})^2}{2d(1+\frac{2B_k}{d})},\qquad \alpha_{k,d}^{+}(U)=\frac{B_k(d+1)(2+U/\gamma_\mathrm{b})^2}{2d(1+\frac{2B_k}{d})}$$

$$\beta_{k,d}^{-}(U)=\frac{1-\frac{B_kU}{d\gamma_\mathrm{b}}}{\sqrt{\frac{1+\frac{2B_k}{d}}{2(d+1)}}},\qquad \beta_{k,d}^{+}(U)=\frac{1+\frac{B_kU}{d\gamma_\mathrm{b}}}{\sqrt{\frac{1+\frac{2B_k}{d}}{2(d+1)}}}.$$

Approximations in Section 3.2

The probability (6) can be efficiently approximation as,

$$\begin{aligned}\mathrm{P}_1 \approx\; & Q\Big(\sqrt{2\gamma_\mathrm{b}}(\tfrac{U_0}{2\gamma_\mathrm{b}}+1)\Big)+Q\Big(\sqrt{2\gamma_\mathrm{b}}(\tfrac{U_0}{2\gamma_\mathrm{b}}-1)\Big)-Q\Big(\sqrt{2\gamma_\mathrm{b}}(\tfrac{U_1}{2\gamma_\mathrm{b}}+1)\Big)-Q\Big(\sqrt{2\gamma_\mathrm{b}}(\tfrac{U_1}{2\gamma_\mathrm{b}}-1)\Big) \\ & +Q\big(2\sqrt{\gamma_\mathrm{b}}-U_1/\sqrt{\gamma_\mathrm{b}}\big)-Q\big(2\sqrt{\gamma_\mathrm{b}}+U_1/\sqrt{\gamma_\mathrm{b}}\big)-\textstyle\sum_{k=1}^{2}\frac{A_k}{2\sqrt{1+2B_k}}\Big\{\mathrm{e}^{-\alpha_{k,1}^{+}(U_0)\gamma_\mathrm{b}}\big\{\mathrm{erf}\Big(\theta_{k,1}^{+-}(U_0)\sqrt{\gamma_\mathrm{b}}\Big) \\ & +\mathrm{erf}\Big(\theta_{k,1}^{-+}(U_0)\sqrt{\gamma_\mathrm{b}}\Big)\big\}+\mathrm{e}^{-\alpha_{k,1}^{-}(U_0)\gamma_\mathrm{b}}\big\{\mathrm{erf}\Big(\theta_{k,1}^{++}(U_0)\sqrt{\gamma_\mathrm{b}}\Big)+\mathrm{sign}(\mu(U_0))\,\mathrm{erf}\Big(\theta_{k,1}^{--}(U_0)\sqrt{\gamma_\mathrm{b}}\Big)\big\}\Big\}\end{aligned}$$

where the auxiliary functions,

$$\theta_{k,d}^{+-}(U)=\frac{\frac{U_D}{2\sqrt{\gamma_\mathrm{b}}}+\frac{1}{\sqrt{N_o}}+\frac{B_k(U_D-U)}{d\sqrt{\gamma_\mathrm{b}}}}{\frac{1+\frac{2B_k}{d}}{(d+1)N_o}},\qquad \theta_{k,d}^{-+}(U)=\frac{\frac{U_D}{2\sqrt{\gamma_\mathrm{b}}}-\frac{1}{\sqrt{N_o}}+\frac{B_k(U_D+U)}{d\sqrt{\gamma_\mathrm{b}}}}{\frac{1+\frac{2B_k}{d}}{(d+1)N_o}}$$

$$\theta_{k,d}^{++}(U)=\frac{\frac{U_D}{2\sqrt{\gamma_\mathrm{b}}}+\frac{1}{\sqrt{N_o}}+\frac{B_k(U_D+U)}{d\sqrt{\gamma_\mathrm{b}}}}{\frac{1+\frac{2B_k}{d}}{(d+1)N_o}},\quad \theta_{k,d}^{--}(U)=\frac{|\mu(U)|}{2}\sqrt{(d+1)N_o(1+\frac{2B_k}{d})}$$

and

$$\mu(U)=\frac{U_D}{\sqrt{\gamma_\mathrm{b}}}-\frac{\frac{2}{\sqrt{N_o}}+\frac{2B_kU}{\sqrt{\gamma_\mathrm{b}}}}{1+2B_k}.$$

Furthermore, the BER_2 can be approximated as,

$$\begin{aligned}\mathrm{BER}_2 \approx\; & Q\Big(\sqrt{2\gamma_\mathrm{b}}(\tfrac{U_1}{2\gamma_\mathrm{b}}+1)\Big)+Q\big(\sqrt{6\gamma_\mathrm{b}}\big) \\ & -\textstyle\sum_{k=1}^{2}\frac{A_k}{\sqrt{1+B_k}}\Big\{\mathrm{e}^{-\alpha_{k,2}^{-}(U_0)\gamma_\mathrm{b}}Q\Big(\beta_{k,2}^{+}(U_0)\sqrt{\gamma_\mathrm{b}}\Big)+\mathrm{e}^{-\alpha_{k,2}^{+}(U_0)\gamma_\mathrm{b}}Q\Big(\beta_{k,2}^{-}(U_0)\sqrt{\gamma_\mathrm{b}}\Big)\Big\} \\ & +\textstyle\sum_{k=1}^{2}\frac{A_k}{\sqrt{1+2B_k}}\Big\{\mathrm{e}^{-\alpha_{k,1}^{-}(U_0)\gamma_\mathrm{b}}Q\Big(\beta_{k,1}^{+}(U_0)\sqrt{\gamma_\mathrm{b}}\Big)+\mathrm{e}^{-\alpha_{k,1}^{+}(U_0)\gamma_\mathrm{b}}Q\Big(\beta_{k,1}^{-}(U_0)\sqrt{\gamma_\mathrm{b}}\Big) \\ & \qquad -\mathrm{e}^{-\alpha_{k,1}^{-}(U_1)\gamma_\mathrm{b}}Q\Big(\beta_{k,1}^{+}(U_1)\sqrt{\gamma_\mathrm{b}}\Big)-\mathrm{e}^{-\alpha_{k,1}^{+}(U_1)\gamma_\mathrm{b}}Q\Big(\beta_{k,1}^{-}(U_1)\sqrt{\gamma_\mathrm{b}}\Big)\Big\}.\end{aligned}$$

BER approximation in Section 3.3

The BER_D can be accurately approximated as,

$$\begin{aligned}\mathrm{BER}_D \approx\ & Q\Big(\sqrt{2\gamma_\mathrm{b}}\left(\tfrac{U_{D-1}}{2\gamma_\mathrm{b}}+1\right)\Big)+Q\Big(\sqrt{2\gamma_\mathrm{b}(D+1)}\Big)-\textstyle\sum_{k=1}^{2}\frac{A_k}{\sqrt{1+\frac{2B_k}{D}}}\Big\{\mathrm{e}^{-\alpha^{-}_{k,D}(U_0)\gamma_\mathrm{b}}Q\Big(\beta^{+}_{k,D}(U_0)\sqrt{\gamma_\mathrm{b}}\Big)\\ &+\mathrm{e}^{-\alpha^{+}_{k,D}(U_0)\gamma_\mathrm{b}}Q\Big(\beta^{-}_{k,D}(U_0)\sqrt{\gamma_\mathrm{b}}\Big)\Big\}+\textstyle\sum_{i=1}^{D-1}\sum_{k=1}^{2}\frac{A_k}{\sqrt{1+\frac{2B_k}{i}}}\Big\{\mathrm{e}^{-\alpha^{-}_{k,i}(U_{D-i-1})\gamma_\mathrm{b}}Q\Big(\beta^{+}_{k,i}(U_{D-i-1})\sqrt{\gamma_\mathrm{b}}\Big)\\ &+\mathrm{e}^{-\alpha^{+}_{k,i}(U_{D-i-1})\gamma_\mathrm{b}}Q\Big(\beta^{-}_{k,i}(U_{D-i-1})\sqrt{\gamma_\mathrm{b}}\Big)-\mathrm{e}^{-\alpha^{-}_{k,i}(U_{D-i})\gamma_\mathrm{b}}Q\Big(\beta^{+}_{k,i}(U_{D-i})\sqrt{\gamma_\mathrm{b}}\Big)\\ &-\mathrm{e}^{-\alpha^{+}_{k,i}(U_{D-i})\gamma_\mathrm{b}}Q\Big(\beta^{-}_{k,i}(U_{D-i})\sqrt{\gamma_\mathrm{b}}\Big)\Big\}.\end{aligned}$$

BER approximation in Section 3.4

Assuming the integral approximations given above, the average BER over a slowly fading channel after D retransmissions can be approximated as,

$$\begin{aligned}\overline{\mathrm{BER}}_D \approx\ & 1-\tfrac{1}{2}\left(\tfrac{4}{\bar{\gamma}_\mathrm{b}(U_{D-1}/\gamma_\mathrm{b}+2)^2}+1\right)^{-1/2}-\tfrac{1}{2}\left(1+\tfrac{1}{\bar{\gamma}_\mathrm{b}(D+1)}\right)^{-1/2}\\ &+\sum_{k=1}^{2}\frac{A_k}{\sqrt{1+\frac{2B_k}{D}}}\Bigg\{\left(1+\bar{\gamma}_\mathrm{b}\Big(\alpha^{-}_{k,D}(U_0)+\tfrac{\beta^{+}_{k,D}(U_0)}{\sqrt{2}}\big(\tfrac{\beta^{+}_{k,D}(U_0)}{\sqrt{2}}+\sqrt{\tfrac{1}{\bar{\gamma}_\mathrm{b}}+\alpha^{-}_{k,D}(U_0)+\tfrac{\beta^{+}_{k,D}(U_0)^2}{2}}\big)\Big)\right)^{-1}\\ &+\left(1+\bar{\gamma}_\mathrm{b}(\alpha^{+}_{k,D}(U_0)+\tfrac{\beta^{-}_{k,D}(U_0)}{\sqrt{2}}\big(\tfrac{\beta^{-}_{k,D}(U_0)}{\sqrt{2}}+\sqrt{\tfrac{1}{\bar{\gamma}_\mathrm{b}}+\alpha^{+}_{k,D}(U_0)+\tfrac{\beta^{-}_{k,D}(U_0)^2}{2}}\big)\right)^{-1}\Bigg\}+\sum_{i=1}^{D-1}\sum_{k=1}^{2}\frac{A_k}{\sqrt{1+\frac{2B_k}{i}}}\times\\ &\times\Bigg\{\left(1+\bar{\gamma}_\mathrm{b}\Big(\alpha^{-}_{k,i}(U_{D-i-1})+\tfrac{\beta^{+}_{k,i}(U_{D-i-1})}{\sqrt{2}}\big(\tfrac{\beta^{+}_{k,i}(U_{D-i-1})}{\sqrt{2}}+\sqrt{\tfrac{1}{\bar{\gamma}_\mathrm{b}}+\alpha^{-}_{k,i}(U_{D-i-1})+\tfrac{\beta^{+}_{k,i}(U_{D-i-1})^2}{2}}\big)\Big)\right)^{-1}\\ &+\left(1+\bar{\gamma}_\mathrm{b}\Big(\alpha^{+}_{k,i}(U_{D-i-1})+\tfrac{\beta^{-}_{k,i}(U_{D-i-1})}{\sqrt{2}}\big(\tfrac{\beta^{-}_{k,i}(U_{D-i-1})}{\sqrt{2}}+\sqrt{\tfrac{1}{\bar{\gamma}_\mathrm{b}}+\alpha^{+}_{k,i}(U_{D-i-1})+\tfrac{\beta^{-}_{k,i}(U_{D-i-1})^2}{2}}\big)\Big)\right)^{-1}\\ &-\left(1+\bar{\gamma}_\mathrm{b}\Big(\alpha^{-}_{k,i}(U_{D-i})+\tfrac{\beta^{+}_{k,i}(U_{D-i})}{\sqrt{2}}\big(\tfrac{\beta^{+}_{k,i}(U_{D-i})}{\sqrt{2}}+\sqrt{\tfrac{1}{\bar{\gamma}_\mathrm{b}}+\alpha^{-}_{k,i}(U_{D-i})+\tfrac{\beta^{+}_{k,i}(U_{D-i})^2}{2}}\big)\Big)\right)^{-1}\\ &-\left(1+\bar{\gamma}_\mathrm{b}\Big(\alpha^{+}_{k,i}(U_{D-i})+\tfrac{\beta^{-}_{k,i}(U_{D-i})}{\sqrt{2}}\big(\tfrac{\beta^{-}_{k,i}(U_{D-i})}{\sqrt{2}}+\sqrt{\tfrac{1}{\bar{\gamma}_\mathrm{b}}+\alpha^{+}_{k,i}(U_{D-i})+\tfrac{\beta^{-}_{k,i}(U_{D-i})^2}{2}}\big)\Big)\right)^{-1}\Bigg\}.\end{aligned}$$

Acknowledgment

This work was supported by Aselsan A.S. and the graduate scholarship from Saudi Arabia.

Disclosure statement

The author(s) declare(s) no potential conflict of interest regarding the publication of this paper.

References

[1] A. Goldsmith, P. Varaiya, Capacity of fading channels with channel side information, IEEE Trans. Inform. Theory 43 (6) (1997) 1986–1992.

[2] T. M. Cover, J. A. Thomas, Elements of Information Theory, 2nd Edition, John Wiley & Sons, 1991.

[3] J. G. Proakis, Digital Communications, 4th Edition, McGraw-Hill, 2001.

[4] S. Lin, D. J. Costello, Error Control Coding: Fundamentals and Applications, Prentice-Hall, 1983.

[5] 5GAA, An assessment of LTE-V2X (PC5) and 802.11p direct communications technologies for improved road safety in the EU (Dec. 2017).

[6] J. Pirskanen et al., On future enhancements to 802.11 technology, tech. Report (Mar. 2013).

[7] J. C. Ikuno, M. Wrulich, M. Rupp, Performance and modeling of LTE H-ARQ, in: ITG Workshop, 2009, pp. 1–6.

[8] K. C. Beh, A. Doufexi, S. M. D. Armour, Performance evaluation of hybrid ARQ schemes of 3GPP LTE OFDMA system, in: Proc. PIMRC, 2007, pp. 1–5.

[9] G. Wang, J. Wu, Y. R. Zheng, Optimum energy- and spectral-efficient transmissions for delay-constrained hybrid ARQ systems, IEEE Trans. Vehic. Tech. 65 (7) (2016) 5212–5221.

[10] E. Modiano, An adaptive algorithm for optimizing the packet size used in wireless ARQ protocols, Wireless Nets. 5 (1999) 279–286.

[11] B. Makki, A. G. i Amat, T. Eriksson, On noisy ARQ in block-fading channels, IEEE Trans. Vehic. Tech. 63 (2) (2014) 731–746.

[12] R. A. Ahmad, J. Lacan, F. Arnal, M. Gineste, L. Clarac, Enhancing satellite system throughput using adaptive HARQ for delay tolerant services in mobile communications, in: WTS, 2015, pp. 1–7.

[13] T. Ji, W. Stark, Rate-adaptive transmission over correlated fading channels, IEEE Trans. Commun. 53 (10) (2005) 1663–1670.

[14] A. Ahmed, Z. Muhammad, H. Mahmood, N. A. Saqib, Partial automatic repeat request transceiver for bandwidth and power efficient multiple-input multiple-output orthogonal frequency division multiplexing systems, IET Commun. 9 (4) (2015) 476–486.

[15] H. T. Pai, Y. S. Han, Y. J. Chu, New HARQ scheme based on decoding of tail-biting convolutional codes in IEEE 802.16e, IEEE Trans. Vehic. Tech. 60 (3) (2011) 912–918.

[16] C. Wengerter, A. G. E. von Elbwart, E. Seidel, G. Velev, M. Schmitt, Advanced hybrid ARQ technique employing a signal constellation rearrangement, in: Proc. VTC, Vol. 4, 2006, pp. 2002–2006.

[17] J. Jung, H. Park, J. Lim, A novel hybrid ARQ scheme based on shift column permutation bit interleaving for OFDM systems, in: Proc. VTC, 2006, pp. 1–5.

[18] H. Chen, R. G. Maunder, L. Hanzo, A survey and tutorial on low-complexity turbo coding techniques and a holistic hybrid ARQ design example 15 (4) (2013) 1546–1566.

[19] D. E. Lucani, M. Médard, M. Stojanovic, On coding for delay-network coding for time-division duplexing, IEEE Trans. Inform. Theory 58 (4) (2012) 2330–2348.

[20] A. Moreira, D. E. Lucani, Coded schemes for asymmetric wireless interfaces: Theory and practice, IEEE J. Select. Areas Commun. 33 (2) (2015) 171–184.

[21] M. Jabi, A. E. Hamss, L. Szczecinski, P. Piantanida, Multipacket hybrid ARQ: Closing gap to the ergodic capacity, IEEE Trans. Commun. 63 (12) (2015) 5191–5205.

[22] E. Malkamäki, H. Leib, Performance of truncated type-II hybrid ARQ schemes with noisy feedback over block fading channels, IEEE Trans. Commun. 48 (9) (2000) 1477–1487.

[23] M. A. M. Hassanien, P. Loskot, Improving link reliability complexity trade-off by exploiting reliable feedback signaling, in: Proc. ISWCS, 2010, pp. 775–779.

[24] E. Biglieri, Coding for Wireless Channels (Information Technology: Transmission, Processing and Storage), Springer-Verlag, Berlin, Heidelberg, 2005.

[25] D. Knuth, The Art of Computer Programming, Addison-Wesley, 1998.

[26] P. Loskot, N. C. Beaulieu, Prony and polynomial approximations for evaluation of the average probability of error over slow-fading channels, IEEE Trans. Vehic. Tech. 58 (3) (2009) 119–138.

[27] M. Petrova, J. Riihijarvi, P. Mahonen, S. Labella, Performance study of IEEE 802.15.4 using measurements and simulations, in: Proc. WCNC, Vol. 1, 2006, pp. 487–492.

Mohamed Hassanien obtained B.Eng. with the highest honors from the AAST University, Egypt in 2003, and M.Sc. with distinction and Ph.D. degrees from Swansea University, UK in 2007 and 2011, respectively. In 2011 and 2012, he was a principal researcher in the British Telecom Plc. funded project on traffic modeling and evaluation in broadband networks. He then held several academic and industrial positions in the Middle East countries. His current research interests involve physical layer problems in wireless and photonics networks.

Pavel Loskot (SM'IEEE) is a Senior Lecturer in the College of Engineering at Swansea University in the United Kingdom. He has obtained long term study and work experience from the Czech Republic, Finland, Canada, United Kingdom and China. Over the past 20 years he has worked with diverse range of institutions as well as large and small companies. His current research projects include tactical wireless networks, Internet access in remote areas, signal processing problems in computational biology, and system engineering problems in renewable energy and air transportation. He received the best paper awards from Chinacom 2012 and InAir 2016, and delivered keynotes and tutorial talks on various topics in numerous international conferences.

Mr. Salman M. Al-Shehri has over 20 years of direct hands-on experience with deployment, and operation of military communications systems. He has been involved in the spectrum management and planning for tactical networks, simulations of combat radio networks, and the design of DSR systems. He was a technical supervisor and a committee member in a number of military communications projects, and delivered several courses on tactical networks previously. Currently, he is finishing his PhD degree at Swansea University, UK.

Dr. Tolga Numanoglu received the B.Sc. degree with the highest honors from the Middle East Technical University, Ankara, Turkey in 2003 followed by the M.Sc. and Ph.D. degrees from the University of Rochester, USA, in 2004 and 2009, respectively. Since December 2009, he has been with Aselsan in Ankara, Turkey, where he now holds the position of the Lead Software Design Engineer. His primary research interests include wireless military communications, ad hoc and sensor networks, signal processing, and information theory.

Mr. Mehmet Mert is with Aselsan, Ankara, Turkey, where he is involved in the management of a portfolio of collaborative and commercial projects.

Mohamed Hassanien

Pavel Loskot

Salman Alshehri

Tolga Numanoglu

Mehmet Mert

PHYCOM_2019_115
Bitwise Retransmission Schemes for Wireless Sensor Networks

Conflict of Interest

The authors declare no potential conflict of interest regarding the publication of this paper.